Top-down modulation of sensory cortex gates perceptual learning

Melissa L. Caras[a,1] and Dan H. Sanes[a,b,c,d]

[a]Center for Neural Science, New York University, New York, NY 10003; [b]Department of Psychology, New York University, New York, NY 10003; [c]Department of Biology, New York University, New York, NY 10003; and [d]Neuroscience Institute, New York University Langone Medical Center, New York, NY 10016

Edited by Ranulfo Romo, Universidad Nacional Autonóma de México, Mexico City, Mexico, and approved August 1, 2017 (received for review July 11, 2017)

Practice sharpens our perceptual judgments, a process known as perceptual learning. Although several brain regions and neural mechanisms have been proposed to support perceptual learning, formal tests of causality are lacking. Furthermore, the temporal relationship between neural and behavioral plasticity remains uncertain. To address these issues, we recorded the activity of auditory cortical neurons as gerbils trained on a sound detection task. Training led to improvements in cortical and behavioral sensitivity that were closely matched in terms of magnitude and time course. Surprisingly, the degree of neural improvement was behaviorally gated. During task performance, cortical improvements were large and predicted behavioral outcomes. In contrast, during nontask listening sessions, cortical improvements were weak and uncorrelated with perceptual performance. Targeted reduction of auditory cortical activity during training diminished perceptual learning while leaving psychometric performance largely unaffected. Collectively, our findings suggest that training facilitates perceptual learning by strengthening both bottom-up sensory encoding and top-down modulation of auditory cortex.

learning | plasticity | top-down | cortex | auditory

A broad range of sensory skills improve with practice during perceptual learning (PL), including language acquisition (1–3), musical abilities (4), and recognition of emotions (5). The neural bases for such perceptual improvement may vary widely. For example, training-based changes in neural activity have been identified in a number of brain regions, including early (6–13) and late (14, 15) sensory cortices, multisensory regions (16, 17), and downstream decision-making areas (18). Similarly, several neural mechanisms have been proposed, such as enhanced signal representation (19), reduction of external (20, 21) or internal (22, 23) noise, and improvement in sensory readout or decision making (13, 18, 24, 25).

The apparent divergence of loci and mechanisms associated with PL could be due, in part, to limitations of experimental design. For example, some neural changes associated with PL are transient (26–29), making it necessary to monitor neural activity throughout the duration of perceptual training, rather than making comparisons only after PL is complete (6–12, 14–16, 30). For similar reasons, it is critical to block the function of a specific candidate brain region during training to determine whether it plays a causal role in PL. Although some reports show that manipulating brain activity can influence PL (28, 31–34), there are no loss-of-function experiments to determine whether a particular region is required for behavioral improvement.

To address these unresolved issues, we recorded from auditory cortex (ACx) as animals improved on an auditory detection task and, in separate experiments, blocked ACx activity during the period of perceptual training. We found that neural and behavioral sensitivity improved in a nearly identical manner over the course of training, in terms of both absolute magnitude and kinetics. Furthermore, reversible down-regulation of ACx activity reduced learning without grossly impairing perception, suggesting that a critical amount of ACx activity is required for PL. Finally, the magnitude of ACx plasticity depended strongly on task performance. We propose an inclusive conceptual framework that acknowledges a role for plasticity within both the ascending sensory neuraxis and descending modulatory pathways.

Results

We trained Mongolian gerbils on an amplitude modulation (AM) detection task (Fig. 1*A*), a perceptual skill that displays significant improvement in humans (35). Animals were trained to drink from a water spout while in the presence of the "safe" stimulus (unmodulated noise), and to withdraw from the spout when the sound changed to the "warn" stimulus (0 dB relative to 100% depth, 5-Hz AM noise), to avoid an aversive shock. All animals learned this procedure quickly, reaching our performance criterion ($d' > 1.5$) within four training sessions (2.1 ± 0.18 sessions, n = 16 animals across all experiments; see *SI Appendix*, *Materials and Methods*). To determine whether this auditory percept required ACx activity, we infused a high dose of muscimol (1 mg/mL; 1 μL per hemisphere; total dose of 2 μg) bilaterally in four animals (*SI Appendix*, Fig. S1*A*). At this concentration, muscimol significantly impaired AM detection ($P = 0.0006$; *SI Appendix*, Fig. S1*B*) by reducing hit rates ($P < 0.0001$; *SI Appendix*, Fig. S1*C*) without increasing false alarm rates ($P = 0.63$; *SI Appendix*, Fig. S1*D*).

To verify that our task was well-suited to assess perceptual learning, we quantified behavioral performance across daily training sessions. During these sessions, we presented warn stimuli of varying AM depths (*SI Appendix*, Figs. S2 and S3) to obtain psychometric functions and derive AM detection thresholds (AM depth at $d' = 1$; *SI Appendix*, *Materials and Methods*). AM depth

Significance

With training, stimulus detection or discrimination abilities can improve dramatically. This process, called perceptual learning, supports language acquisition, musical expertise, and professional judgments, such as the identification of abnormalities in X-rays. To explore neural mechanisms that support perceptual learning, we measured and manipulated auditory cortex activity as animals trained on an auditory task. We found improvements in neural sensitivity that correlated tightly with perceptual learning, both in absolute magnitude and time course, and depended strongly on task engagement. Disrupting auditory cortical function impaired learning while leaving perception largely intact. Our findings indicate that improvements in cortical sensitivity could plausibly explain perceptual learning, and suggest that plasticity within top-down networks may be a general mechanism for perceptual improvement.

Author contributions: M.L.C. and D.H.S. designed research; M.L.C. performed research; M.L.C. analyzed data; and M.L.C. and D.H.S. wrote the paper.

The authors declare no conflict of interest.

This article is a PNAS Direct Submission.

Data deposition: Data and analysis code can be found at https://nyu.box.com/v/caras-sanes-2017.

[1]To whom correspondence should be addressed. Email: caras@nyu.edu.

This article contains supporting information online at www.pnas.org/lookup/suppl/doi:10.1073/pnas.1712305114/-/DCSupplemental.

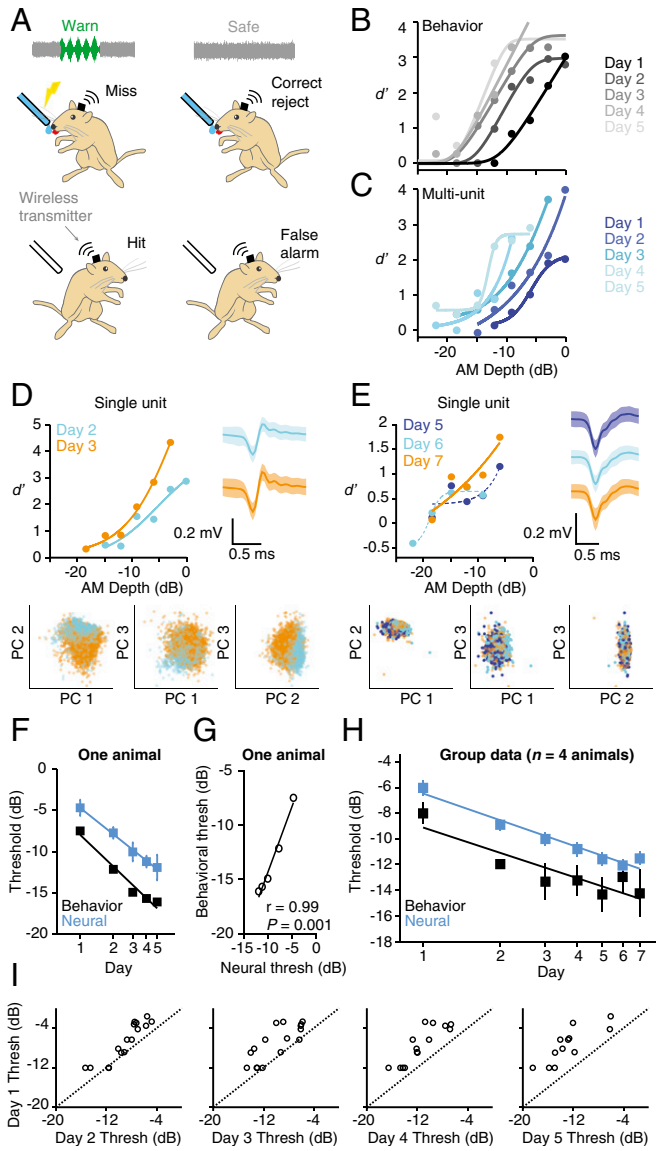

Fig. 1. Cortical and behavioral improvements are similar in magnitude and time course. (*A*) Wireless recordings were made from ACx of animals as they performed an AM detection task. (*B*) Psychometric functions from one animal improved across days. Data from this animal are presented in *C*–*G*. (*C*) Neurometric functions from one multiunit recorded during task performance improved across days. (*D*) Neurometric performance for a single unit held across multiple sessions improved from day 2 (cyan) to day 3 (orange). Single-unit identity was confirmed by stable waveform shape [compare waveforms from day 2 (cyan) and day 3 (orange); *Right*]. Waveforms represent mean ± 2 SDs. Single-unit identity was also confirmed by the fact that waveforms from day 2 and day 3 clustered tightly together within principal component (PC) space (*Bottom*). (*E*) Data from another single unit held across multiple training sessions. Plot conventions are as in *D*. Dashed lines indicate fits that did not yield valid thresholds. (*F*) Mean ± SEM neural and behavioral sensitivity improve simultaneously in one animal ($n = 30$ sites; 4 to 7 per d). (*G*) Behavioral and neural thresholds of one animal are tightly correlated. (*H*) Mean ± SEM neural and behavioral thresholds improve simultaneously across all animals and units [neural: $F_{6,224} = 16$, $P < 0.0001$, $n = 231$ (range: 29 to 39 sites per d; *SI Appendix*, Table S1); behavior: $F_{4,12} = 11$, $P = 0.0005$, $n = 4$ animals]. (*I*) Day 1 vs. day 2 to 5 thresholds of units recorded over multiple days. See *SI Appendix*, Table S3 for statistics. The dashed lines are unity.

detection improved during training, as shown for one representative animal in Fig. 1*B*. These improvements were due to increased hit rates (*SI Appendix*, Fig. S4*A*) rather than decreased false alarm rates (*SI Appendix*, Fig. S4*B*). Importantly, the hit rate for the largest AM depth tested (0 dB) was maximal on day 1 and remained steady on day 2, suggesting that the animals began perceptual training when already at perceptual asymptote for this stimulus value (*SI Appendix*, Fig. S4*A*). Additionally, the hit rates for shallow depths improved more gradually than for higher depths. These observations are consistent with the finding that PL progresses systematically from easy to difficult stimuli (36), and support the idea that our experimental paradigm specifically assessed PL, rather than associative or procedural learning.

To determine whether there is a temporal correlation between neural and behavioral improvement, we implanted animals with chronic electrode arrays and recorded single- and multiunit activity in left ACx as animals trained and improved on the AM detection task ($n = 231$ AM-responsive sites; $n = 4$ animals; *SI Appendix*, *Materials and Methods* and Table S1). We found that training improved neural performance, both at the multi- and single-unit level (Fig. 1 *C*–*E*). These improvements occurred in concert with behavior, such that the average firing rate (FR)-based neural sensitivity closely tracked psychometric sensitivity on a day-to-day basis (Fig. 1*F*). As illustrated in Fig. 1*G* for one representative animal, the majority (3/4) of our subjects showed a significant correlation between neural and behavioral thresholds (*SI Appendix*, Table S2). The distribution of correlation regression slopes did not differ significantly from a distribution centered around 1 (0.92 ± 0.10, $t_3 = -0.76$, $P = 0.50$, $n = 4$), indicating that the ACx population threshold is a good predictor of perceptual sensitivity. At the group level, perceptual training had a significant effect on both neural ($P < 0.0001$) and behavioral thresholds ($P = 0.0005$), with improvement occurring at similar rates [neural, −7.0; behavioral, −6.6 dB/log(day); Fig. 1*H*]. In the one animal that we followed for 14 training days, neural improvement was maintained after perceptual performance reached asymptote (*SI Appendix*, Fig. S5).

In visual cortex, training-induced changes are often most pronounced in specific subpopulations of neurons (7, 14, 15). To determine whether a similarly selective mechanism operates in ACx, we examined thresholds for recording sites that were held across multiple training days. As shown in Fig. 1*I*, nearly all sites demonstrated significant training-induced improvement, regardless of starting threshold (day 1 vs. day 2 to 5 thresholds: all $P < 0.001$; see *SI Appendix*, Table S3 for details). This finding suggests that training may enhance sensitivity across the population of AM-responsive sites, rather than acting selectively on a restricted subset of units. It is important to note, however, that training could differentially affect units with different tuning properties, which were not systematically characterized here because many neurons failed to respond when animals were not engaged in the task.

Improvements in neural sensitivity could be due to an increased separation of warn- and safe-evoked FR distributions (13), and/or a reduction in FR variability across training days (20–23, 37). As illustrated for one representative multiunit in Fig. 2*A*, warn and safe FR distributions gradually separated during training without a systematic change in the unit's mean FR or trial-to-trial variability (measured by the coefficient of variation; CV). To quantify this effect across our population, we calculated an FR ratio (AM-evoked FR/unmodulated FR) for each unit on each training day. FR ratios steadily increased across days, leading to a larger separation between AM and unmodulated FRs (all $P < 0.0001$; Fig. 2*B*). In contrast, CVs remained stable throughout training (all $P > 0.05$; Fig. 2*C*), as did population FRs (all $P > 0.05$; see *SI Appendix*, Fig. S6 for a full explanation). These findings suggest that PL is supported by a gradual separation of the warn and safe FR distributions, rather than a reduction in response variability.

Behavioral evidence suggests that top-down processes, such as attention, arousal, and motivation, can facilitate or enable PL (12, 38–43). Here, we adopt the term "top-down" to mean the

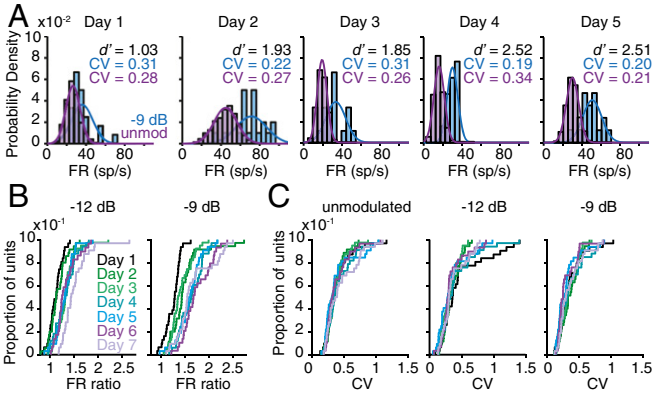

Fig. 2. PL is supported by an increasing separation of the warn and safe FR distributions. (*A*) Warn (−9-dB AM) and safe (unmodulated) FR distributions from one representative multiunit show increasing separation during training. sp, spikes. (*B*) Perceptual training increases FR ratios across the population (−12 dB: $H = 59.2$, $P < 0.0001$; −9 dB: $H = 65.8$, $P < 0.0001$). (*C*) Perceptual training does not affect CV [unmodulated: $H = 3.61$, $P = 0.73$; −12 dB: $H = 5.12$, $P = 0.53$; −9 dB: $H = 7.25$, $P = 0.30$]. In *B* and *C*, $n = 231$ (range: 29 to 39 sites per d; *SI Appendix*, Table S1).

functional influence of a descending projection from one or more brain regions on neural activity in sensory cortex. A commonly used procedure to assess the magnitude of top-down mechanisms is to compare neural responsiveness during two different states of behavioral engagement (37, 44–49). Specifically, top-down inputs are thought to actively modulate ACx responses during task performance (or "engagement") but not during nontask ("disengaged") listening sessions (50, 51). Thus, the difference between engaged and disengaged sensitivity is a proxy for the strength of a top-down mechanism. We used this approach to examine whether training affects the magnitude of a top-down mechanism during PL. Specifically, we recorded ACx activity during disengaged listening sessions that occurred just before ("pre") and just after ("post") training sessions. During these disengaged sessions, the spout and metal floorplate were removed from the test cage; otherwise, the sound stimuli presented and the position of the recording electrodes were identical to behaviorally engaged sessions.

As training progressed, three outcomes were possible (*SI Appendix*, Fig. S7). If training does not affect the strength of a top-down mechanism, then the difference between engaged and disengaged AM sensitivity should remain constant, despite training-based improvement. Alternatively, if training weakens the strength of a top-down mechanism, the difference between engaged and disengaged AM sensitivity should become smaller. This scenario could occur if training allows sensory processing to become more automatic, as previously proposed (26, 52, 53). Finally, if training strengthens a top-down mechanism, such as attention (54, 55), the difference between engaged and disengaged AM sensitivity should become larger during PL.

Throughout training, a smaller proportion of units responded to AM during disengaged sessions compared with engaged sessions (all $P < 0.001$; *SI Appendix*, Tables S1 and S4), and those that did respond during disengaged sessions had poorer thresholds ($P = 0.0022$; Fig. 3 *A* and *B*). This weak sensitivity was due to reduced AM-evoked discharge rates during disengagement ($P < 0.001$; Fig. 3*C* and *SI Appendix*, Figs. S2 and S3). These state-dependent changes in AM sensitivity were not explained by recording instability, as FRs evoked by unmodulated noise did not differ significantly across conditions ($P = 0.095$; Fig. 3*C*).

As training progressed, disengaged neural thresholds displayed a modest improvement but did not correlate with behavioral thresholds, as illustrated for a single animal in Fig. 3 *D* and *E* (group data in *SI Appendix*, Table S2; all *P* values are nonsignificant). Moreover, at the group level, the rate of disengaged improvement, while significant (all $P < 0.05$), was >50% slower than that observed during task engagement [pre, −3.2; engaged, −7.0; post, −2.4 dB/log(day); Fig. 3*F*]. As a result, the difference between engaged and disengaged neural thresholds grew larger as training progressed (compare beginning and ending orange brackets in Fig. 3*F*). Similar findings were observed using a timing-based analysis of AM-evoked activity (*SI Appendix*, Fig. S8). Collectively, these findings suggest that training strengthens both bottom-up inputs to and top-down modulation of ACx, which together give rise to PL (Fig. 3*G*).

To determine whether ACx activity is required for PL, we assessed baseline behavioral performance in a separate group of animals ($n = 6$) and then paired perceptual training with bilateral ACx infusions of muscimol or saline (Fig. 4*A* and *SI Appendix*, Fig. S9). To distinguish the role of ACx in perceptual learning from its

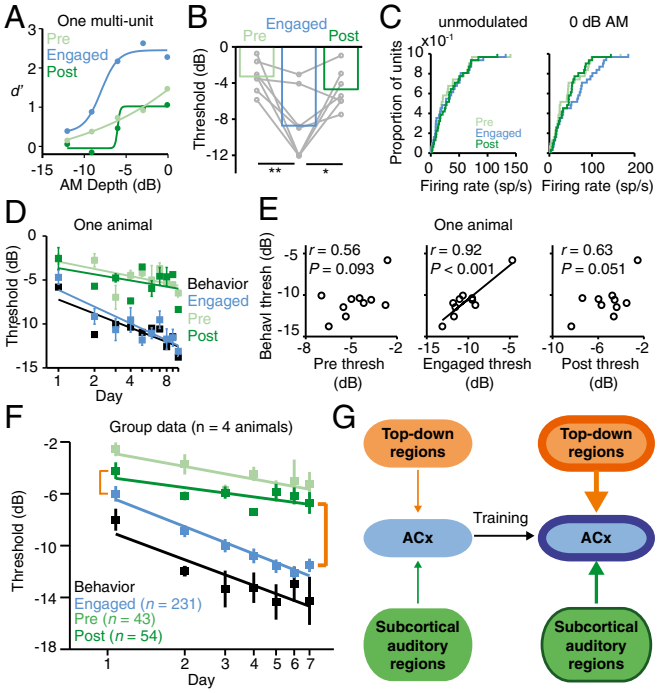

Fig. 3. Behaviorally gated neural plasticity increases during PL. (*A*) Day 1 performance of one multiunit. (*B*) Task engagement improves day 1 neural thresholds ($F_{2,12} = 11$, $P = 0.0022$; pre vs. engaged: $t_6 = 3.8$, $P = 0.0093$; post vs. engaged: $t_6 = 2.7$, $P = 0.034$; $n = 7$). Only units that responded under all conditions were included. (*C*) Task engagement does not affect day 1 unmodulated FRs [$X^2(2) = 4.71$, $P = 0.095$] but increases AM-evoked FRs [$X^2(2) = 15.3$, $P < 0.001$; pre vs. engaged: $Z = -4.12$, $P < 0.001$; post vs. engaged: $Z = -3.67$, $P < 0.001$]. All $n = 31$. (*D*) Mean ± SEM neural thresholds of one animal improve more quickly during task engagement than during disengaged listening [pre: $n = 2$ to 4 sites per d (32 total); engaged: $n = 7$ to 11 sites per d (86 total); post: $n = 1$ to 4 sites per d (23 total)]. (*E*) Neural thresholds correlate with behavioral thresholds in one animal (same subject as in *D*) only during task engagement. (*F*) Across all animals, mean ± SEM neural thresholds from disengaged listening sessions improve with training (pre: $F_{6,37} = 4.3$, $P = 0.0021$, $n = 2$ to 11 sites per d; post: $F_{6,54} = 3.0$, $P = 0.014$, $n = 4$ to 14 sites per d; *SI Appendix*, Table S1), but improvement is slower than during task engagement. The strength of top-down ACx modulation is reflected by the difference between engaged and disengaged thresholds (orange brackets). Engaged neural and behavioral data are replotted from Fig. 1*H*. (*G*) Model in which training induces plasticity in both bottom-up (thick green outline and arrow) and top-down (thick orange outline and arrow) pathways, leading to improved ACx sensory sensitivity (thick blue outline) that supports PL.

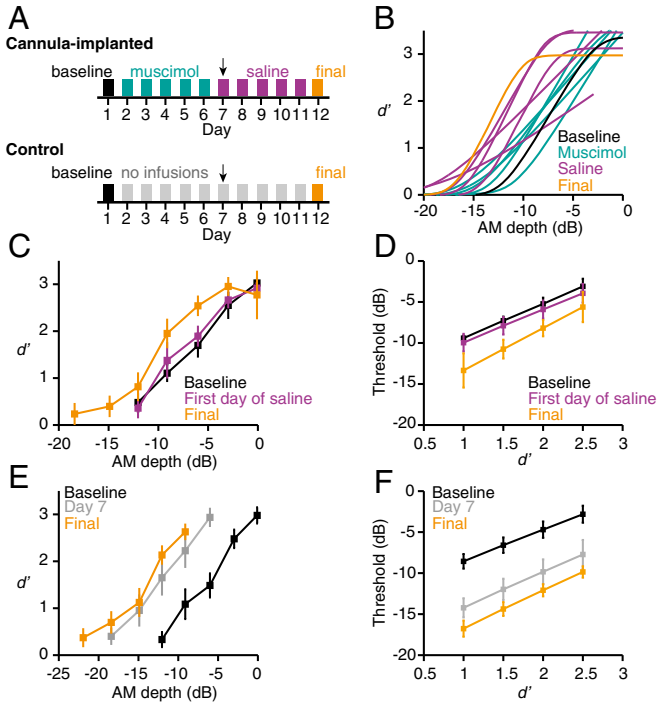

Fig. 4. Reduced ACx activity disrupts PL. (*A*) Experimental timeline for cannula-implanted animals (*Top*) and unimplanted controls (*Bottom*). Arrows highlight the middle time point analyzed in *C* and *D* (first day of saline) and *E* and *F* (day 7). Muscimol dose used in these experiments was 1 μg (0.5 mg/mL; 1 μL per hemisphere). (*B*) Psychometric fits from one representative cannula-implanted animal during perceptual training. (*C* and *D*) Time point has a significant effect on (*C*) mean ± SEM d' values ($F_{2,10} = 7.2$, $P = 0.012$) and (*D*) mean ± SEM thresholds extracted at different d' values ($F_{2,10} = 5.5$, $P = 0.025$) from cannula-implanted animals ($n = 6$). (*E* and *F*) Time point has a significant effect on (*E*) mean ± SEM d' values ($F_{2,10} = 15$, $P = 0.001$) and (*F*) mean ± SEM thresholds ($F_{1.1,5.4} = 18$, $P = 0.006$) from control animals ($n = 6$). Note that in *C* and *E*, we do not display points for which we had data from only a single animal.

role in perception, it was important to identify a dose of muscimol that did not grossly perturb psychometric performance on the AM detection task. We found that 0.5 mg/mL (1 μL per hemisphere; total dose of 1 μg) allowed for excellent detection of 0-dB AM (*SI Appendix*, Fig. S10) and relatively unimpaired psychometric performance in the majority of our animals (*SI Appendix*, Fig. S11; $P = 0.073$). Furthermore, this dose had no effect on trial completion rates, false alarm rates, or reaction times (all $P > 0.05$; *SI Appendix*, Fig. S12), implying that motor processes and response biases were not impacted by the treatment. Thus, we used this dose to ask whether ACx activity is required for PL.

As illustrated for one animal in Fig. 4*B*, behavioral performance remained stable throughout muscimol-paired sessions (also see *SI Appendix*, Fig. S11) but demonstrated steady improvement during subsequent sessions paired with saline. To quantify this observation at the group level, we compared behavioral performance at three time points: (*i*) baseline before perceptual training, (*ii*) the first day of saline infusion, and (*iii*) the final training session. If muscimol prevents PL, rather than simply impairing AM sensitivity, we would expect behavioral performance to be similar at baseline and the first day of saline infusion. As predicted, values obtained at baseline and on the first day of saline infusion largely overlapped. Final d' values were higher, however, indicating improved perceptual performance ($P = 0.012$; Fig. 4*C*). To confirm that this effect was robust, we extracted AM depth thresholds for each animal at four different d' values. As shown in Fig. 4*D*, final AM thresholds were lower than those obtained at baseline or during the first day of saline infusion ($P = 0.025$).

During muscimol infusion experiments, we controlled for the amount of daily practice by limiting animals to 50 warn trials per session (see *SI Appendix*, *Materials and Methods* for the rationale). Thus, it was possible that the lack of improvement between baseline and the first day of saline infusion was not due to a muscimol-induced learning impairment but instead to insufficient practice. To rule out this possibility, a separate group of control animals ($n = 6$) received perceptual training for 12 d with 50 warn trials per session, identical to the muscimol group (Fig. 4*A*). As shown in Fig. 4*E*, d' values were higher on day 7 than at baseline, and approached those obtained on the final training day ($P = 0.001$). Similarly, thresholds were lower at day 7 and day 12 compared with baseline ($P = 0.006$; Fig. 4*F*). Collectively, these results show that reducing ACx activity during perceptual training prevents learning.

Discussion

PL is closely associated with long-term changes in sensory cortex activity (6–15, 56, 57), and these changes may contribute to learning (28, 31–34). However, no studies have tested whether sensory cortex is necessary for PL. Here, we found that bilateral ACx infusion of a low dose of muscimol could prevent practice-based improvement. We interpret this result to mean that the manipulation permitted enough ACx activity to allow for task performance across a range of AM depths but not enough to enable the plasticity mechanisms required for PL. This interpretation is consistent with a model of PL which posits that, in order for plasticity to occur, sensory-evoked activity must surpass a threshold for learning (58, 59). It is important to note, however, that muscimol disrupted psychometric performance to a greater degree in two of our six subjects (*SI Appendix*, Fig. S11). Thus, in these two animals, it is possible that a degraded sensory representation also contributed to impaired learning. Our findings are in line with previous manipulations that dissociated auditory processing from a learning mechanism. For example, song learning in juvenile zebra finches is diminished by administration of an NMDA receptor antagonist during a developmental sensory acquisition phase, even though the drug does not alter auditory brainstem responses (60) or song discrimination (61).

The results of our muscimol inactivation experiments indicate that proper ACx activity is required for PL. Consistent with this finding, we observed a tight correlation between ACx and behavioral plasticity throughout perceptual training, in terms of both magnitude and kinetics (Fig. 1*H*). The neural basis of PL has commonly been evaluated by focusing on two time points (pre- vs. posttraining) or groups (trained vs. untrained) (6–12, 14–16, 30). However, training-based perceptual improvement can be associated with transient phases of functional plasticity, even within a single network (26–29). Thus, studies that are restricted to one or two time points could fail to identify a temporary contribution of a particular brain region to PL. A handful of studies have recorded neural responses during the full time course of visual perceptual training; however, direct comparisons of neural and perceptual improvement either (*i*) were restricted to early and late time points (56, 57), (*ii*) revealed relatively weak neural improvements (13), or (*iii*) resulted in modest correlations between neural and behavioral plasticity (18). In contrast, we found that ACx neurons displayed substantial day-to-day improvements in neural sensitivity that were tightly correlated with, and could plausibly explain, PL.

AM-evoked responses in ACx are enhanced during task performance. This result is in line with an abundance of work demonstrating behaviorally gated modulations of ACx activity (37, 44–49, 62–66). Our observation that disengaged neural sensitivity is better if measured immediately after behavioral testing, rather than before (compare green lines in Fig. 3*F*), is consistent with an effect of task-specific plasticity that persists

after the behavioral session has concluded. For example, Fritz et al. found that task-dependent spectrotemporal receptive field plasticity in ACx persists for minutes to hours after behavioral performance (47). Similarly, passive stimulus exposure has been found to facilitate PL if the exposure occurs within a short window following active practice (67), presumably when task-dependent neural enhancements are still operational (58, 59). It should be noted, however, that we cannot rule out the possibility that the enhancements we observed during behavioral performance were the result of non–task-specific arousal mechanisms (68, 69).

A distinguishing feature of our results is that the effect of task engagement increases in magnitude across perceptual training sessions. During task performance, neural improvements were pronounced and tightly correlated with perceptual abilities. During nontask listening sessions, however, neural improvements were present but weak, and were uncorrelated with behavior. These findings led us to propose an inclusive conceptual framework: Specifically, we posit that training induces plasticity within the top-down networks that modulate stimulus-driven activity during task performance, thereby augmenting bottom-up plasticity within sensory cortex.

Evidence for bottom-up plasticity derives from previous experiments in which animals were trained on an auditory detection or discrimination task and then anesthetized for extracellular recordings after reaching perceptual asymptote. These studies report that trained animals display altered auditory cortical responses, such as tonotopic reorganization (9, 12) and enhanced AM processing (10, 11). Similarly, Adab and colleagues recorded from V4 and posterior inferior temporal cortex neurons of awake monkeys during training on an orientation discrimination task (57, 70). The authors found that training enhanced the responses to the orientation gratings, and the enhancements were present both during task performance and during passive fixation. Together, these findings suggest that perceptual training can induce neural changes that are observable even when animals are anesthetized or when the task-relevant stimuli are unattended. Thus, we interpret the small, but significant, neural improvements we observed during task disengagement as reflecting plasticity within a bottom-up pathway.

It is important to recognize, however, that changes in bottom-up stimulus encoding do not explain all forms of PL (6, 56, 71, 72). For example, Gilbert and colleagues found that while perceptual training on an embedded contour detection task has little effect on basic response properties of monkey V1 neurons, it has a pronounced effect on how V1 neurons are modulated by stimulus context (6, 56, 71). This finding stands in contrast to those described above from V4 (57, 70) and primary ACx (9–12), where it was found that training modified stimulus-encoding properties. These apparent dissimilarities may reflect differences among functional networks, behavioral tasks, or species.

Our observation that neural improvements are more pronounced during task performance is consistent with the well-established finding that top-down processes known to modulate sensory cortex activity also facilitate and guide PL (12, 17, 38–43). For our purposes, top-down refers to the functional influence of a higher-order brain region on neural activity in ACx, brought about by task engagement. Several plausible candidate regions may mediate this top-down effect, either in isolation or in concert with one another, including frontal cortex (50, 51), nucleus basalis (73–75), locus coeruleus (76), ventral tegmental area (77, 78), and multisensory cortex (17).

Current models of PL suggest that top-down inputs act to restrict task-dependent plasticity to the appropriate neurons (79–83) or enhance stimulus signals above some threshold beyond which plasticity mechanisms are operational (58, 59). Our hypothesis is consistent with these models but posits that, rather than providing a static modulatory signal, top-down networks change throughout training, thereby contributing to improved ACx sensitivity and PL. This framework is similar to a computational model that has been proposed to explain visual brightness discrimination learning (84) and is consistent with human psychophysical and imaging evidence that training can improve visual attentional modulation (55, 85, 86) and general cognitive skills (23). Thus, training-induced plasticity in top-down modulatory processes may be a general mechanism that supports PL across sensory modalities.

Materials and Methods

Subjects. Adult Mongolian gerbils (*Meriones unguiculatus*) were raised from commercially obtained breeding pairs (Charles River). Animals were housed on a 12-h light/12-h dark cycle and provided with ad libitum food and water unless otherwise noted. All procedures were approved by the Institutional Animal Care and Use Committee at New York University.

Behavior. AM detection was assessed with an aversive conditioning paradigm as described previously (29, 87, 88). Psychometric functions were fit with cumulative Gaussians and transformed to the signal detection metric, d' (89). Threshold was defined as the AM depth at which $d' = 1$, unless otherwise stated.

Electrophysiology. Extracellular single- and multiunit activity was recorded from left ACx as described previously (37, 90). Firing rates were transformed to d' values and fit with logistic functions (37). Units were considered "responsive" if they generated a valid fit and threshold (at $d' = 1$).

Infusions. Guide cannulas (Plastics One) were implanted into bilateral ACx. Animals were anesthetized briefly with isoflurane, and infused with muscimol or saline 45 min before behavioral training.

Statistics. Analyses were performed using JMP (SAS), PASW Statistics (IBM), or SPSS (IBM). When data were not normally distributed, nonparametric tests were used. All reported P values were Holm–Bonferroni–corrected for multiple comparisons.

For full methodological details, see *SI Appendix*. Data and analysis code can be found at https://nyu.box.com/v/caras-sanes-2017.

ACKNOWLEDGMENTS. We thank Derek Wang and Stephen Young for assistance with data collection and histology, and other members of the D.H.S. laboratory for constructive feedback and discussions. Special thanks to Drs. Beverly Wright, Michael Long, Daniel Stolzberg, Jonathan Fritz, and Daniel Polley for helpful discussions and comments on earlier versions of this work. This research was supported by NIH R01DC014656 (to D.H.S.) and NIH K99DC016046 (to M.L.C.).

1. Bradlow AR, Pisoni DB, Akahane-Yamada R, Tohkura Y (1997) Training Japanese listeners to identify English /r/ and /l/: IV. Some effects of perceptual learning on speech production. *J Acoust Soc Am* 101:2299–2310.
2. Kuhl PK, et al. (2006) Infants show a facilitation effect for native language phonetic perception between 6 and 12 months. *Dev Sci* 9:F13–F21.
3. Sundara M, Polka L, Genesee F (2006) Language-experience facilitates discrimination of /d-th/ in monolingual and bilingual acquisition of English. *Cognition* 100:369–388.
4. White EJ, Hutka SA, Williams LJ, Moreno S (2013) Learning, neural plasticity and sensitive periods: Implications for language acquisition, music training and transfer across the lifespan. *Front Syst Neurosci* 7:90.
5. Du Y, Zhang F, Wang Y, Bi T, Qiu J (2016) Perceptual learning of facial expressions. *Vision Res* 128:19–29.
6. Crist RE, Li W, Gilbert CD (2001) Learning to see: Experience and attention in primary visual cortex. *Nat Neurosci* 4:519–525.
7. Schoups A, Vogels R, Qian N, Orban G (2001) Practising orientation identification improves orientation coding in V1 neurons. *Nature* 412:549–553.
8. Recanzone GH, Merzenich MM, Jenkins WM, Grajski KA, Dinse HR (1992) Topographic reorganization of the hand representation in cortical area 3b owl monkeys trained in a frequency-discrimination task. *J Neurophysiol* 67:1031–1056.
9. Recanzone GH, Schreiner CE, Merzenich MM (1993) Plasticity in the frequency representation of primary auditory cortex following discrimination training in adult owl monkeys. *J Neurosci* 13:87–103.
10. Beitel RE, Schreiner CE, Cheung SW, Wang X, Merzenich MM (2003) Reward-dependent plasticity in the primary auditory cortex of adult monkeys trained to discriminate temporally modulated signals. *Proc Natl Acad Sci USA* 100:11070–11075.
11. Bao S, Chang EF, Woods J, Merzenich MM (2004) Temporal plasticity in the primary auditory cortex induced by operant perceptual learning. *Nat Neurosci* 7:974–981.

12. Polley DB, Steinberg EE, Merzenich MM (2006) Perceptual learning directs auditory cortical map reorganization through top-down influences. *J Neurosci* 26:4970–4982.
13. Yan Y, et al. (2014) Perceptual training continuously refines neuronal population codes in primary visual cortex. *Nat Neurosci* 17:1380–1387.
14. Yang T, Maunsell JH (2004) The effect of perceptual learning on neuronal responses in monkey visual area V4. *J Neurosci* 24:1617–1626.
15. Raiguel S, Vogels R, Mysore SG, Orban GA (2006) Learning to see the difference specifically alters the most informative V4 neurons. *J Neurosci* 26:6589–6602.
16. Gu Y, et al. (2011) Perceptual learning reduces interneuronal correlations in macaque visual cortex. *Neuron* 71:750–761.
17. Powers AR, III, Hevey MA, Wallace MT (2012) Neural correlates of multisensory perceptual learning. *J Neurosci* 32:6263–6274.
18. Law CT, Gold JI (2008) Neural correlates of perceptual learning in a sensory-motor, but not a sensory, cortical area. *Nat Neurosci* 11:505–513.
19. Gold J, Bennett PJ, Sekuler AB (1999) Signal but not noise changes with perceptual learning. *Nature* 402:176–178.
20. Dosher BA, Lu ZL (1998) Perceptual learning reflects external noise filtering and internal noise reduction through channel reweighting. *Proc Natl Acad Sci USA* 95:13988–13993.
21. Dosher BA, Lu ZL (1999) Mechanisms of perceptual learning. *Vision Res* 39:3197–3221.
22. Jones PR, Moore DR, Amitay S, Shub DE (2013) Reduction of internal noise in auditory perceptual learning. *J Acoust Soc Am* 133:970–981.
23. Amitay S, Zhang YX, Jones PR, Moore DR (2014) Perceptual learning: Top to bottom. *Vision Res* 99:69–77.
24. Petrov AA, Dosher BA, Lu ZL (2005) The dynamics of perceptual learning: An incremental reweighting model. *Psychol Rev* 112:715–743.
25. Law CT, Gold JI (2009) Reinforcement learning can account for associative and perceptual learning on a visual-decision task. *Nat Neurosci* 12:655–663.
26. Sigman M, et al. (2005) Top-down reorganization of activity in the visual pathway after learning a shape identification task. *Neuron* 46:823–835.
27. Yotsumoto Y, Watanabe T, Sasaki Y (2008) Different dynamics of performance and brain activation in the time course of perceptual learning. *Neuron* 57:827–833.
28. Reed A, et al. (2011) Cortical map plasticity improves learning but is not necessary for improved performance. *Neuron* 70:121–131.
29. Sarro EC, von Trapp G, Mowery TM, Kotak VC, Sanes DH (2015) Cortical synaptic inhibition declines during auditory learning. *J Neurosci* 35:6318–6325.
30. Ghose GM, Yang T, Maunsell JH (2002) Physiological correlates of perceptual learning in monkey V1 and V2. *J Neurophysiol* 87:1867–1888.
31. Tegenthoff M, et al. (2005) Improvement of tactile discrimination performance and enlargement of cortical somatosensory maps after 5 Hz rTMS. *PLoS Biol* 3:e362.
32. Karim AA, Schüler A, Hegner YL, Friedel E, Godde B (2006) Facilitating effect of 15-Hz repetitive transcranial magnetic stimulation on tactile perceptual learning. *J Cogn Neurosci* 18:1577–1585.
33. Pleger B, et al. (2006) Repetitive transcranial magnetic stimulation-induced changes in sensorimotor coupling parallel improvements of somatosensation in humans. *J Neurosci* 26:1945–1952.
34. Shibata K, Watanabe T, Sasaki Y, Kawato M (2011) Perceptual learning incepted by decoded fMRI neurofeedback without stimulus presentation. *Science* 334:1413–1415.
35. Fitzgerald MB, Wright BA (2011) Perceptual learning and generalization resulting from training on an auditory amplitude-modulation detection task. *J Acoust Soc Am* 129:898–906.
36. Ahissar M, Hochstein S (1997) Task difficulty and the specificity of perceptual learning. *Nature* 387:401–406.
37. von Trapp G, Buran BN, Sen K, Semple MN, Sanes DH (2016) A decline in response variability improves neural signal detection during auditory task performance. *J Neurosci* 36:11097–11106.
38. Shiu LP, Pashler H (1992) Improvement in line orientation discrimination is retinally local but dependent on cognitive set. *Percept Psychophys* 52:582–588.
39. Ahissar M, Hochstein S (1993) Attentional control of early perceptual learning. *Proc Natl Acad Sci USA* 90:5718–5722.
40. Ito M, Westheimer G, Gilbert CD (1998) Attention and perceptual learning modulate contextual influences on visual perception. *Neuron* 20:1191–1197.
41. Seitz AR, Nanez JE, Sr, Holloway S, Tsushima Y, Watanabe T (2006) Two cases requiring external reinforcement in perceptual learning. *J Vis* 6:966–973.
42. Seitz AR, Kim D, Watanabe T (2009) Rewards evoke learning of unconsciously processed visual stimuli in adult humans. *Neuron* 61:700–707.
43. Mukai I, Bahadur K, Kesavabhotla K, Ungerleider LG (2011) Exogenous and endogenous attention during perceptual learning differentially affect post-training target thresholds. *J Vis* 11:25.
44. Miller JM, et al. (1972) Single cell activity in the auditory cortex of rhesus monkeys: Behavioral dependency. *Science* 177:449–451.
45. Benson DA, Hienz RD, Goldstein MH, Jr (1981) Single-unit activity in the auditory cortex of monkeys actively localizing sound sources: Spatial tuning and behavioral dependency. *Brain Res* 219:249–267.
46. Ryan AF, Miller JM, Pfingst BE, Martin GK (1984) Effects of reaction time performance on single-unit activity in the central auditory pathway of the rhesus macaque. *J Neurosci* 4:298–308.
47. Fritz J, Shamma S, Elhilali M, Klein D (2003) Rapid task-related plasticity of spectrotemporal receptive fields in primary auditory cortex. *Nat Neurosci* 6:1216–1223.
48. Lee CC, Middlebrooks JC (2011) Auditory cortex spatial sensitivity sharpens during task performance. *Nat Neurosci* 14:108–114.
49. Niwa M, Johnson JS, O'Connor KN, Sutter ML (2012) Active engagement improves primary auditory cortical neurons' ability to discriminate temporal modulation. *J Neurosci* 32:9323–9334.
50. Winkowski DE, Bandyopadhyay S, Shamma SA, Kanold PO (2013) Frontal cortex activation causes rapid plasticity of auditory cortical processing. *J Neurosci* 33:18134–18148.
51. Winkowski DE, et al. (January 8, 2017) Orbitofrontal cortex neurons respond to sound and activate primary auditory cortex neurons. *Cereb Cortex*, 10.1093/cercor/bhw409.
52. Vaina LM, Belliveau JW, des Roziers EB, Zeffiro TA (1998) Neural systems underlying learning and representation of global motion. *Proc Natl Acad Sci USA* 95:12657–12662.
53. Mukai I, et al. (2007) Activations in visual and attention-related areas predict and correlate with the degree of perceptual learning. *J Neurosci* 27:11401–11411.
54. Amitay S, Irwin A, Moore DR (2006) Discrimination learning induced by training with identical stimuli. *Nat Neurosci* 9:1446–1448.
55. Byers A, Serences JT (2014) Enhanced attentional gain as a mechanism for generalized perceptual learning in human visual cortex. *J Neurophysiol* 112:1217–1227.
56. Li W, Piëch V, Gilbert CD (2008) Learning to link visual contours. *Neuron* 57:442–451.
57. Adab HZ, Vogels R (2011) Practicing coarse orientation discrimination improves orientation signals in macaque cortical area V4. *Curr Biol* 21:1661–1666.
58. Seitz AR, Dinse HR (2007) A common framework for perceptual learning. *Curr Opin Neurobiol* 17:148–153.
59. Wright BA, Zhang Y (2009) in *The Cognitive Neurosciences*, ed Gazzaniga MS (MIT Press, Cambridge, MA), pp 353–366.
60. Aamodt SM, Nordeen EJ, Nordeen KW (1996) Blockade of NMDA receptors during song model exposure impairs song development in juvenile zebra finches. *Neurobiol Learn Mem* 65:91–98.
61. Basham ME, Nordeen EJ, Nordeen KW (1996) Blockade of NMDA receptors in the anterior forebrain impairs sensory acquisition in the zebra finch (*Poephila guttata*). *Neurobiol Learn Mem* 66:295–304.
62. Fritz JB, Elhilali M, Shamma SA (2005) Differential dynamic plasticity of A1 receptive fields during multiple spectral tasks. *J Neurosci* 25:7623–7635.
63. Fritz JB, Elhilali M, Shamma SA (2007) Adaptive changes in cortical receptive fields induced by attention to complex sounds. *J Neurophysiol* 98:2337–2346.
64. David SV, Fritz JB, Shamma SA (2012) Task reward structure shapes rapid receptive field plasticity in auditory cortex. *Proc Natl Acad Sci USA* 109:2144–2149.
65. Yin P, Fritz JB, Shamma SA (2014) Rapid spectrotemporal plasticity in primary auditory cortex during behavior. *J Neurosci* 34:4396–4408.
66. Buran BN, et al. (2014) A sensitive period for the impact of hearing loss on auditory perception. *J Neurosci* 34:2276–2284.
67. Wright BA, Sabin AT, Zhang Y, Marrone N, Fitzgerald MB (2010) Enhancing perceptual learning by combining practice with periods of additional sensory stimulation. *J Neurosci* 30:12868–12877.
68. Goris RL, Movshon JA, Simoncelli EP (2014) Partitioning neuronal variability. *Nat Neurosci* 17:858–865.
69. McGinley MJ, David SV, McCormick DA (2015) Cortical membrane potential signature of optimal states for sensory signal detection. *Neuron* 87:179–192.
70. Adab HZ, Popivanov ID, Vanduffel W, Vogels R (2014) Perceptual learning of simple stimuli modifies stimulus representations in posterior inferior temporal cortex. *J Cogn Neurosci* 26:2187–2200.
71. Ramalingam N, McManus JN, Li W, Gilbert CD (2013) Top-down modulation of lateral interactions in visual cortex. *J Neurosci* 33:1773–1789.
72. Piëch V, Li W, Reeke GN, Gilbert CD (2013) Network model of top-down influences on local gain and contextual interactions in visual cortex. *Proc Natl Acad Sci USA* 110:E4108–E4117.
73. Froemke RC, Merzenich MM, Schreiner CE (2007) A synaptic memory trace for cortical receptive field plasticity. *Nature* 450:425–429.
74. Froemke RC, et al. (2013) Long-term modification of cortical synapses improves sensory perception. *Nat Neurosci* 16:79–88.
75. Kuchibhotla KV, et al. (2017) Parallel processing by cortical inhibition enables context-dependent behavior. *Nat Neurosci* 20:62–71.
76. Martins AR, Froemke RC (2015) Coordinated forms of noradrenergic plasticity in the locus coeruleus and primary auditory cortex. *Nat Neurosci* 18:1483–1492.
77. Stark H, Scheich H (1997) Dopaminergic and serotonergic neurotransmission systems are differentially involved in auditory cortex learning: A long-term microdialysis study of metabolites. *J Neurochem* 68:691–697.
78. Bao S, Chan VT, Merzenich MM (2001) Cortical remodelling induced by activity of ventral tegmental dopamine neurons. *Nature* 412:79–83.
79. Roelfsema PR, van Ooyen A (2005) Attention-gated reinforcement learning of internal representations for classification. *Neural Comput* 17:2176–2214.
80. Ahissar M, Hochstein S (2004) The reverse hierarchy theory of visual perceptual learning. *Trends Cogn Sci* 8:457–464.
81. Ahissar M, Nahum M, Nelken I, Hochstein S (2009) Reverse hierarchies and sensory learning. *Philos Trans R Soc Lond B Biol Sci* 364:285–299.
82. Gilbert CD, Sigman M (2007) Brain states: Top-down influences in sensory processing. *Neuron* 54:677–696.
83. Kim D, Seitz AR, Watanabe T (2015) Visual perceptual learning by operant conditioning training follows rules of contingency. *Vis Cogn* 23:147–160.
84. Schäfer R, Vasilaki E, Senn W (2007) Perceptual learning via modification of cortical top-down signals. *PLoS Comput Biol* 3:e165.
85. Bartolucci M, Smith AT (2011) Attentional modulation in visual cortex is modified during perceptual learning. *Neuropsychologia* 49:3898–3907.
86. Byers A, Serences JT (2012) Exploring the relationship between perceptual learning and top-down attentional control. *Vision Res* 74:30–39.
87. Heffner HE, Heffner RS (1995) in *Methods in Comparative Psychoacoustics*, eds Klmup GM, Dooling RJ, Fay RR, Stebbins WC (Springer, Basel), pp 79–93.
88. Caras ML, Sanes DH (2015) Sustained perceptual deficits from transient sensory deprivation. *J Neurosci* 35:10831–10842.
89. Green DM, Swets JA (1966) *Signal Detection Theory and Psychophysics* (Wiley, New York).
90. Buran BN, von Trapp G, Sanes DH (2014) Behaviorally gated reduction of spontaneous discharge can improve detection thresholds in auditory cortex. *J Neurosci* 34: 4076–4081.

Supporting Information for:

Top-down modulation of sensory cortex gates perceptual learning

Melissa L. Caras[a,1], Dan H. Sanes[a,b,c]

This PDF file includes:

Materials and Methods

Subjects

Adult Mongolian gerbils (*Meriones unguiculatus*) were raised from commercially obtained breeding pairs (Charles River). Animals were housed on a 12-h light/12-h dark cycle, and provided with *ad libitum* food and water unless otherwise noted. All procedures were approved by the Institutional Animal Care and Use Committee at New York University.

Behavioral Apparatus

Behavioral performance was assessed with a yes-no aversive conditioning paradigm, as described previously (1-5). Briefly, a stainless steel spout was positioned above a metal floorplate within a test cage. Water delivery was initiated by a syringe pump (NE-1000; New Era Pump Systems) triggered by infrared detection at the spout contact. Sound stimuli were delivered from a calibrated free-field speaker (DX25TG05-04; Vifa) positioned 1m in front of the test cage. The cage and speaker were housed within a sound-attenuating room (GretchKen), and monitored remotely. Stimulus delivery and data acquisition were controlled using custom Python scripts (written by Dr. Bradley Buran) and an RZ6 multifunction processor (Tucker Davis Technologies).

Associative Training

Animals were placed on controlled water access, and trained to drink continuously while in the presence of steady, unmodulated, broadband noise (60 dB SPL; 2.5-20 kHz; 12 dB/octave roll-off). Animals learned to withdraw from the spout when the sound changed from the "safe" cue (unmodulated noise) to the "warn" cue (0 dB re: 100% depth sinusoidal AM noise; 5 Hz

modulation rate; 1 s duration) by pairing the warn cue with a mild shock (0.5-1.0 mA, 300 ms; Lafayette Instruments) delivered through the metal lick spout (Fig. 1A). To be consistent with previous literature, and because the decision axis for AM detection is logarithmic (6), depths are presented here on a dB scale (re: 100% depth). Thus, 0 dB (re: 100% depth) refers to fully modulated (100% depth) noise, and negative numbers refer to shallower depths. These dB (re:100% depth) values are not to be confused with dB SPL values, which indicate the root-mean-squared intensity of the stimulus.

Individual animals vary in their sensitivity to pain (7); thus, the shock level was adjusted on a subject-by-subject basis to reliably elicit spout withdrawal, without dissuading the animal from resuming drinking shortly thereafter. Warn trials were interspersed with 3-5 safe trials, during which the unmodulated sound continued unchanged. The unpredictable nature of the warn presentation prevented temporal conditioning. The gain of the AM signal was adjusted to control for changes in average power across modulation depths (6, 8).

Behavioral Scoring

Behavioral responses were scored by monitoring the animal's contact with the spout during the final 100 msec of each trial. Breaking contact for ≥ 50 msec was considered a spout "withdrawal" and was scored as a correct "hit" on warn trials (AM noise), and as an incorrect "false alarm" on safe trials (unmodulated noise; Fig. 1A). Testing began only after an animal had reached a criterion level of behavioral performance ($d' \geq 1.5$ for 0 dB depth; see Psychometric Analysis below). On the final day of associative training, and throughout testing, the root-mean-squared stimulus intensity was held constant at 45 dB SPL.

47 Psychometric Training and Testing

48 Each psychometric session began with a series of "reminder trials" at 0 dB depth. After the
49 animal responded correctly to 3 consecutive reminder stimuli (or consumed 0.5 mL of water,
50 whichever came first), psychometric assessment commenced. Five AM depths (Figs. S2-S3)
51 were presented in descending order (interspersed with 3-5 safe trials, as described above).

52 Animals underwent perceptual training for 5-14 days. Sessions took place every 24 to 48
53 hours. The five depths presented during the first psychometric session (0, -3, -6, -9 and -12 dB
54 re: 100%) were chosen because they bracketed naive AM depth detection thresholds, as
55 determined previously (2, 3, 5). The five AM depths presented in each subsequent session were
56 determined by the animal's performance on the previous day. Consecutive AM depths were
57 always in increments of 3 dB.

58 Maintaining threshold bracketing within and across sessions made it likely that animals
59 would fail to detect the smallest of the AM depths presented. Delivering shocks during such
60 trials would likely lead to a cessation of drinking, or intermittent pecking at the spout, which
61 would result in an excessively high false alarm rate. To avoid these possibilities, the shock was
62 turned off for the lowest two depths presented. A previous study (9) validated the necessity of
63 this approach, and confirmed that animals do not become conditioned to the presence or absence
64 of the shock.

65

66 Psychometric Analysis

67 The percent of "yes" responses (spout withdrawals) was plotted as function of modulation
68 depth. These psychometric functions were fit with a cumulative Gaussian using the maximum

likelihood procedure of the open-source package psignifit 4 for MATLAB (10). The formula for this function is as follows:

$$\Psi(x,m,w,\gamma,\lambda) = \gamma + (1-\gamma-\lambda)S(x;m,w) \quad (1)$$

where

$$S(x;m,w) = \Phi\left(C\frac{(x-m)}{w}\right) \text{ and } C = \Phi^{-1}(0.95) - \Phi^{-1}(0.5) \quad (2)$$

Here, Φ and Φ^{-1} represent the cumulative standard normal distribution and its inverse, x represents the modulation depth, m the threshold, λ the lapse rate, γ the false alarm rate, and w the width of the interval over which $S(x;m,w)$ rises from γ to λ.

Bayesian inference was used to obtain parameter estimates for a beta-binomial model; thus prior distributions were required for each parameter described above, as well as an additional parameter, η, which represents overdispersion. We used the default priors in Psignifit 4, which worked well for fitting our data. Thus, for m and w, uniform prior distributions were generated automatically from the x values in our dataset, and the prior distributions for γ, λ, and η were defined as beta-distributions with the parameters (1,10) (10).

Fits were transformed to the signal detection metric d' (11):

$$d' = Z(h) - Z(fa) \quad (3)$$

Here, h and fa represent the hit rate and false alarm rate, respectively. To avoid d' values that approach infinity, we set a floor (0.05) and ceiling (0.95) on hit rates and false alarm rates. For each psychometric fit, threshold was defined as the AM depth at which $d' = 1$, unless otherwise stated.

Electrode Implantation Surgery

Animals (n = 4 males) were anesthetized with isoflurane/O_2 and secured in a stereotaxic device (Kopf). An incision was made along the midline, and the skin and fascia were removed. The skull was exposed and dried with H_2O_2. Bone screws were inserted into both frontal bones and the right parietal bone. A craniotomy was made in the left parietal bone, dorsal and medial to auditory cortex. A 4 shank silicone probe array with 16 channels arranged in a 600 x 600 μm grid (A4x4-4mm-200-200-1250-H16_21mm; NeuroNexus) was fixed to a custom-made microdrive to allow for subsequent advancement, and angled 25 degrees in the mediolateral plane. The rostral-most shank of the array was positioned 3.9 mm rostral and 4.8 mm lateral to lambda, and inserted into left core auditory cortex (Fig. S13). Left auditory cortex was targeted because of its sensitivity to time-varying signals, including vocalizations, relative to the right hemisphere (12-14). A ground wire was inserted in the right caudal hemisphere, and the apparatus was secured to the skull via dental acrylic. Animals were allowed to recover for at least 1 week before being placed on controlled water access.

Neurophysiology

Recordings were made in awake animals before, during, and after behavioral sessions using previously described methodology (15, 16). Briefly, extracellular single- and multi-unit activity

was acquired via a 15-channel wireless headstage and receiver (W16; Triangle BioSystems). Analog signals were preamplified, digitized at a 24.414 kHz sampling rate (TB32; Tucker Davis Technologies, TDT), and fed via fiber optic link to an RZ5 base station (TDT) for filtering and processing. To reduce noise, the recordings from all but one channel (e.g. channels 2-15) were averaged together and subtracted from the remaining channel (e.g. channel 1). This method of common average referencing was applied to each channel individually (17). Offline, signals were high-pass filtered (300 Hz; 48 dB/octave roll-off), and a representative 16 sec recording segment was used to estimate the standard deviation (SD) of the background noise, using the algorithm described by Quiroga and colleagues (18). A spike extraction threshold was set 4-5 SDs above the noise floor, and an artifact rejection threshold was set to 20 SDs. Extracted spike waveforms were peak-aligned, hierarchically clustered, and sorted in principal component (PC) space using the MATLAB-based package UltraMegaSort 2000 (19) (Fig. S14). Single-units were characterized by clear separation in PC space, $\leq 10\%$ of spikes violating the refractory period, and $\leq 5\%$ spikes missing, as estimated from a Gaussian fit of the spike amplitude histogram (19) (Fig. S14). Recordings that did not meet these criteria were considered multi-units. Because of the small number of AM-responsive single-units in our dataset (see Table S1), we pooled single- and multi-units together for all group analyses reported here.

During behavioral recording sessions, the number of trials per session was unlimited, and AM depth values were adjusted within each session to maintain threshold bracketing (5). This approach allowed us to maximize our neurophysiological data collection each day.

Recordings were made both during task performance (the “engaged” condition), and during disengaged sessions that occurred just prior to (“pre”) and just after (“post”) the engaged sessions. The number of presentations for each warn depth (averaged across sessions) was

similar across listening conditions [pre: 16 ± 0.22; engaged: 16 ± 0.53; post: 15 ± 0.24; mean ± sem trials].

Neurometric Analysis

The firing rate (spikes/s) of each recording site was calculated over a 1 second duration for both unmodulated and AM noise. Firing rate-based d' values were calculated as:

$$d' = \frac{2\left(\mu FR_{AM} - \mu FR_{UNMOD}\right)}{\sigma FR_{AM} + \sigma FR_{UNMOD}} \quad (4)$$

where μFR_{AM} and σFR_{AM} are the mean and standard deviation of the firing rate for a single modulation depth, and μFR_{UNMOD} and σFR_{UNMOD} represent the mean and standard deviation of the firing rate elicited by the unmodulated noise.

Neural d' values were fit with a logistic function using a nonlinear least-squares regression procedure using the MATLAB function *nlinfit* (Mathworks) (16). The formula for this function is as follows:

$$F(x) = y_0 + \frac{a}{1 + \exp\left(-\left(x - x_0\right)/b\right)} \quad (5)$$

Here, y_0 represents the minimum d' value, x the modulation depth, a the range of d' values, x_0 the modulation depth at the inflection point, and b the slope of the function. The validity of each fit was assessed by calculating the statistical significance of the correlation (Pearson's r) between predicted and actual d' values. For each neurometric fit, threshold was defined as the

AM depth at which $d' = 1$. Units were considered responsive to AM stimuli if they generated a valid neurometric fit and threshold. Units were considered unresponsive if either (i) the fit was deemed invalid, or (ii) the highest d' elicited was below a value of 1. For units with valid fits and a minimum d' value above 1, threshold was set to the lowest AM depth presented in the session.

Cannula Implantation Surgery

Surgical procedures for cannula implantation were similar to those for electrode implantation, described above. After exposing and drying the skull, bone screws were inserted into both frontal bones. Craniotomies were made in the both parietal bones, dorsal and medial to each auditory cortex. Double guide cannula (26 gauge, 3 mm cannula length, 1.2 mm center-to-center distance; C235GS-5-1.2/SPC; Plastics One) were angled 20 degrees in the mediolateral plane. The mediolateral angle of electrodes and cannulas differed because the size of the cannulas prevented bilateral implants angled at 25 degrees. However, histology confirmed that our infusions were centered within ACx (Fig. S9). The rostral most cannula in each hemisphere was positioned 3.9 mm rostral and 4.8 mm lateral to lambda. Cannulas were inserted into left and right core auditory cortices, and the apparatus was secured to the skull via dental acrylic. Dummy cannulas (33 gauge, 3.2 mm cannula length, C235DCS-5/SP; Plastics One) were inserted to keep guides clear and were secured in place with a brass dustcap (303DC/1B; Plastics One). Animals were allowed to recover for at least 1 week before being placed on controlled water access.

Cannula Infusions

Muscimol (AbCam) was dissolved in 0.9% NaCl to achieve a concentration of 4 mg/mL. Aliquots (20-30 μL) were stored at -20°C and used within 1 week. Prior to infusions, aliquots were thawed to room temperature and diluted to 1 (Fig. S1) or 0.5 mg/mL (Fig. 4 and Fig. S11-12) with 0.9% NaCl.

Animals (n = 7 males) were anesthetized with isoflurane/O_2. Dust caps and dummy cannulas were removed from the guides. Infusion cannulas (33 gauge, 4 mm cannula length, C235IS-5/SP; Plastics One) were connected to PE-50 tubing (A-M Systems), backfilled with mineral oil, and connected to glass syringes (10 μL, 1801 Gastight, Hamilton) via 23s gauge needles (Hamilton). Muscimol or saline was drawn into the tip of each infusion cannula, and inserted into the guides. Bilateral infusions (1 μL/hemisphere, 0.2 μL/min) were made simultaneously using a six-channel programmable pump (NE-1600, New Era). Infusion success was confirmed by visually monitoring the movement of the meniscus between the infusion solution (muscimol or saline) and the mineral oil. To ensure full diffusion of the solution, infusion cannulas were left in place for 4 minutes before replacing dummy cannulas and caps. The entire process (from anesthesia induction to cap replacement) took 10-12 minutes. Animals recovered in their home cage for 45 minutes prior to behavioral training or testing. During this time, we observed animals to verify that they were alert and engaged, displayed proper posture, and demonstrated normal motor functions. One of the seven animals did not meet these criteria, and was therefore removed from the study. This animal was the smallest of the infusion group (55.5 gm), weighing >1.5 standard deviations below the mean of the remaining animals (69.5 +/- 8.7 gm).

The 6 remaining animals were used to determine whether ACx activity is necessary for PL (Fig. 4A-D and Fig. S11). Four of these animals were also used to determine whether ACx is necessary for detection of fully modulated AM noise (Fig. S1 and Fig. S10). These latter

experiments took place immediately after associative training was completed, prior to any psychometric training or testing.

When determining whether ACx was required for AM depth detection (Fig. S1), the warn stimulus (0 dB re: 100% depth) was presented a maximum of 20 times per session. During experiments exploring whether ACx activity is necessary for PL (Fig. 4, Figs. S11-S12), each depth was presented a maximum of 10 times. Given enough time or practice, animals with inactivated or lesioned brain regions may develop compensatory neural strategies to solve perceptual tasks (20, 21). In pilot experiments, we found that limiting sessions to 50 total trials minimizes compensation (not shown).

Histology

At the end of all experiments, animals were deeply anesthetized with an intraperitoneal injection of sodium pentobarbital (150 mg/kg) and perfused with phosphate-buffered saline and 4% paraformaldehyde. To mark recording sites in electrode-implanted animals, electrolytic lesions were made by passing current (7 mA, 10 sec) through one contact immediately before perfusion. To estimate the spread of muscimol diffusion in cannula-implanted animals, animals were infused with Fluoro-Ruby (10,000 MW Tetramethylrhodamine dextran, Thermo Fisher; 1μL /hemisphere) 30 – 90 minutes before perfusion. Brains were post-fixed and sectioned at 60 μm on a benchtop vibratome (Leica). Alternate sections from cannula-implanted animals were cleared and coverslipped for fluorescent imaging. All other sections were stained for Nissl. Brightfield and fluorescent images were acquired at 2X and 10X using a high-resolution slide scanner (Olympus). To verify recordings and infusions targeted core auditory cortex, electrode

tracks (Fig. S13) and dye spread (Fig. S9) were reconstructed offline and compared to a gerbil brain atlas (22).

Statistical Analysis

Statistical analyses were performed using JMP 9.0.1 (SAS), PASW Statistics 18.0, or SPSS Statistics 24.0. For normally distributed data (as assessed by the Shaprio-Wilk test), data are reported as mean ± sem unless otherwise stated. When data were not normally distributed, non-parametric analyses were used. In instances of multiple comparisons, alpha values were Holm-Bonferroni-corrected. When violations of sphericity were present, *P* values and degrees of freedom were Greenhouse-Geisser corrected.

For our physiology experiments, animals received perceptual training for either 5, 7, 10, or 14 days (each $n = 1$). We therefore restricted our group analyses to the first 7 days of training for which we had data from $n = 3$ animals. When performing within-subject analyses (such as in Fig. 1F-G, Fig. 3D-E, and Fig. S5), we used all data available. To quantify the correlation between neural and behavioral thresholds within individual animals (Fig. 1G, Fig. 3E and Table S2), we calculated Pearson's *r* and its associated *P* value.

The electrode position within each animal was advanced or kept steady based on the quality and number of AM-responsive recording sites on a given day. As a result of this approach, some sites were recorded over multiple training days, and other sites were only recorded on a single day. Thus, to quantify the overall effect of training on neural thresholds we chose to treat each recording site independently. We therefore used standard 1-way (non repeated-measures, RM) ANOVAs to analyze the neural data depicted in Fig. 1H, Fig 3F, Fig. S5 and Fig. S8.

To assess the effect of training on behavioral thresholds and false alarm rates (Fig. 1H and Fig. S4B), we performed two tests. First, missing values from one animal on days 6 and 7 prevented us from performing RM-ANOVAs for all 7 training days; thus, we performed 1-way RM-ANOVAs across only the first 5 days. Second, we performed less sensitive 1-way (non RM) ANOVAs for all 7 days of testing. As similar effects of training day were found for both tests, we only report the values for the RM-ANOVAs.

Similarly, because AM depths were systematically adjusted to maintain threshold bracketing (see Psychometric Training and Testing, above) some AM depth values were not presented on every test day. These missing values prevented us from performing RM-ANOVAs to test the effect of test day on hit rates (Fig. S4A). We therefore performed 1-way (non RM) ANOVAs for each stimulus value.

To calculate the rate of neural and behavioral improvement, we plotted data on an *x*-log scale, and fit data with a linear regression using the MATLAB functions *polyfit* and *polyval*. The slopes of these lines were taken as our measure of rate of improvement (Fig. 1H and Fig 3F).

To compare thresholds across days within individual units (Fig. 1I and Table S3), we used Student's paired two-tailed *t*-tests.

Because FRs were non-normally distributed, we used Kruskal-Wallis tests to analyze the effect of perceptual training on FR (Fig. S6A), FR standard deviations (Fig. S6B), FR ratios (Fig. 2B), and CV (Fig. 2C). We used the Friedman test and Wilcoxon Signed Ranks tests to compare firing rates across listening conditions (Fig. 3C).

We used a 1-way RM-ANOVA and Student's paired two-tailed *t*-tests to compare neural thresholds between disengaged (pre and post) and engaged listening conditions (Fig. 3B).

To examine the effect of a high dose of muscimol on detection of fully modulated (0 dB re: 100% depth) noise (Fig. S1), we used a 1-way RM-ANOVA. Post-hoc comparisons were performed with Student's paired two-tailed *t*-tests. To determine whether the effect of muscimol on 0 dB AM detection was dose-dependent (Fig. S10), we performed Student's paired two-tailed *t*-tests.

To determine whether a low dose of muscimol affected psychometric performance during training (Fig. S11), we performed a 2-way (stimulus x condition) RM-ANOVA. To determine whether muscimol infusions impaired PL, we examined the effect of time point (baseline, day 7, final) on behavioral *d'* values (Fig. 4C and 4E). Because we maintained threshold bracketing (see Psychometric Training and Testing, above), some AM depth values were not presented at every time point. We took two approaches to analyze data with missing values. First, we created restricted datasets by removing any AM depth value for which we had missing data. Second, we created complete datasets by filling in missing points with *d'* values extrapolated from the psychometric fitted functions. We then analyzed both the restricted and complete datasets using 2-way (time point x AM depth) RM-ANOVAs. Because these analyses yielded qualitatively similar results, we report only the test-statistics and *P* values from the analysis of the complete datasets here. We also used 2-way RM-ANOVAs to determine the effect of time point on thresholds obtained at 4 different *d'* cuts (1, 1.5, 2 and 2.5; Fig 4D and 4F).

To verify that muscimol-induced disruptions of PL were not due to task-specific impairments (such as reduced motivation or disrupted motor function) we examined the effect of ACx infusions on the rate of trial completion, false alarm rates, and reaction times using 1-way RM-ANOVAs (Fig. S12).

References

1. Heffner HE, and Heffner RS (1995) in *Methods in comparative psychoacoustics*, editor Klmup GM, Dooling RJ, Fay RR, and Stebbins WC (Springer, Basel, Switzerland), p 79-93.

2. Sarro EC, and Sanes DH (2010) Prolonged maturation of auditory perception and learning in gerbils. *Dev Neurobiol* 70:636-48.

3. Sarro EC, and Sanes DH (2011) The cost and benefit of juvenile training on adult perceptual skill. *J Neurosci* 31:5383-91.

4. Sarro EC, von Trapp G, Mowery TM, Kotak VC, and Sanes DH (2015) Cortical Synaptic Inhibition Declines during Auditory Learning. *J Neurosci* 35:6318-25.

5. Caras ML, and Sanes DH (2015) Sustained Perceptual Deficits from Transient Sensory Deprivation. *Journal of Neuroscience* 35:10831-10842.

6. Wakefield GH, and Viemeister NF (1990) Discrimination of modulation depth of sinusoidal amplitude modulation (SAM) noise. *J Acoust Soc Am* 88:1367-73.

7. Mogil JS (1999) The genetic mediation of individual differences in sensitivity to pain and its inhibition. *Proc Natl Acad Sci U S A* 96:7744-51.

8. Viemeister NF (1979) Temporal modulation transfer functions based upon modulation thresholds. *J Acoust Soc Am* 66:1364-80.

9. Buran BN, Sarro EC, Manno FA, Kang R, Caras ML, and Sanes DH (2014) A sensitive period for the impact of hearing loss on auditory perception. *J Neurosci* 34:2276-84.

10. Schütt HH, Harmeling S, Macke JH, and Wichmann FA (2016) Painfree and accurate Bayesian estimation of psychometric functions for (potentially) overdispersed data. *Vision Res* 122:105-23.

11. Green DM, and Swets JA (1966) *Signal Detection Theory and Psychophysics* (Wiley, New York).

12. Heffner HE, and Heffner RS (1984) Temporal lobe lesions and perception of species-specific vocalizations by macaques. *Science* 226:75-6.

13. Jamison HL, Watkins KE, Bishop DV, and Matthews PM (2006) Hemispheric specialization for processing auditory nonspeech stimuli. *Cereb Cortex* 16:1266-75.

14. Wetzel W, Ohl FW, and Scheich H (2008) Global versus local processing of frequency-modulated tones in gerbils: an animal model of lateralized auditory cortex functions. *Proc Natl Acad Sci U S A* 105:6753-8.

15. Buran BN, von Trapp G, and Sanes DH (2014) Behaviorally gated reduction of spontaneous discharge can improve detection thresholds in auditory cortex. *J Neurosci* 34:4076-81.

16. von Trapp G, Buran BN, Sen K, Semple MN, and Sanes DH (2016) A Decline in Response Variability Improves Neural Signal Detection during Auditory Task Performance. *J Neurosci* 36:11097-11106.

17. Ludwig KA, Miriani RM, Langhals NB, Joseph MD, Anderson DJ, and Kipke DR (2009) Using a common average reference to improve cortical neuron recordings from microelectrode arrays. *J Neurophysiol* 101:1679-89.

18. Quiroga RQ, Nadasdy Z, and Ben-Shaul Y (2004) Unsupervised spike detection and sorting with wavelets and superparamagnetic clustering. *Neural Comput* 16:1661-87.

19. Hill DN, Mehta SB, and Kleinfeld D (2011) Quality metrics to accompany spike sorting of extracellular signals. *J Neurosci* 31:8699-705.

20. Depner M, Tziridis K, Hess A, and Schulze H (2014) Sensory cortex lesion triggers compensatory neuronal plasticity. *BMC Neurosci* 15:57.

21. Kato HK, Gillet SN, and Isaacson JS (2015) Flexible Sensory Representations in Auditory Cortex Driven by Behavioral Relevance. *Neuron* 88:1027-39.

22. Radtke-Schuller S, Schuller G, Angenstein F, Grosser OS, Goldschmidt J, and Budinger E (2016) Brain atlas of the Mongolian gerbil (Meriones unguiculatus) in CT/MRI-aided stereotaxic coordinates. *Brain Struct Funct* 221 Suppl 1:1-272.

23. Fritz J, Shamma S, Elhilali M, and Klein D (2003) Rapid task-related plasticity of spectrotemporal receptive fields in primary auditory cortex. *Nat Neurosci* 6:1216-23.

24. Fritz JB, Elhilali M, and Shamma SA (2005) Differential dynamic plasticity of A1 receptive fields during multiple spectral tasks. *J Neurosci* 25:7623-35.

25. Fritz JB, Elhilali M, and Shamma SA (2007) Adaptive changes in cortical receptive fields induced by attention to complex sounds. *J Neurophysiol* 98:2337-46.

26. McGinley MJ, Vinck M, Reimer J, Batista-Brito R, Zagha E, Cadwell CR, Tolias AS, Cardin JA, and McCormick DA (2015) Waking State: Rapid Variations Modulate Neural and Behavioral Responses. *Neuron* 87:1143-61.

27. Goris RL, Movshon JA, and Simoncelli EP (2014) Partitioning neuronal variability. *Nat Neurosci* 17:858-65.

28. Kleinfeld D, Sachdev RN, Merchant LM, Jarvis MR, and Ebner FF (2002) Adaptive filtering of vibrissa input in motor cortex of rat. *Neuron* 34:1021-34.

29. Rosen MJ, Semple MN, and Sanes DH (2010) Exploiting development to evaluate auditory encoding of amplitude modulation. *J Neurosci* 30:15509-20.

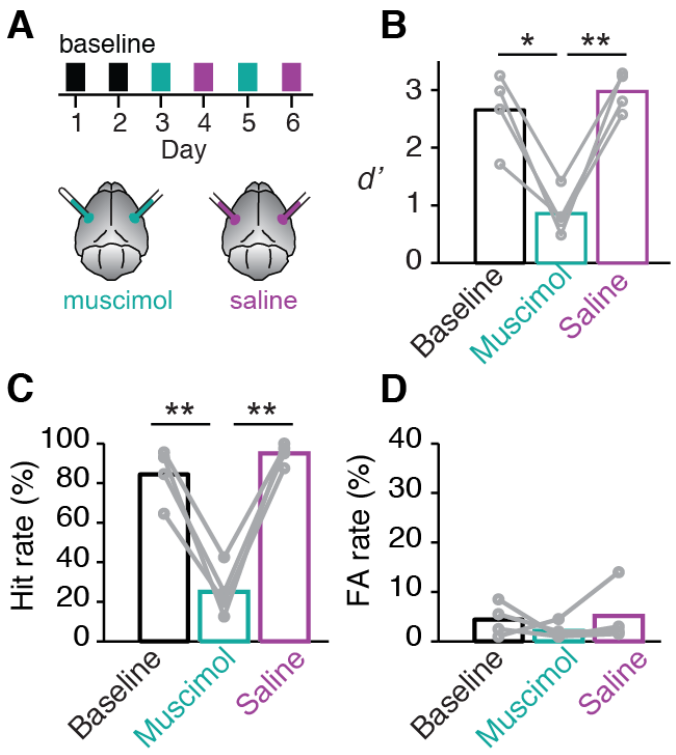

Fig. S1. Auditory cortex activity is necessary for AM detection

(A) Animals (n = 4) were implanted with cannulas into bilateral auditory cortex, and tested on their ability to detect fully modulated (0 dB re: 100%) AM noise using the task schematized in Fig. 1A. (Note that these animals were not implanted with chronic electrode arrays for wireless recording.) After 2 days of baseline testing, animals received bilateral infusions (1µL/hemisphere) of either a high dose of muscimol (1mg/mL; total dose of 2 µg) or saline on alternate days. **(B)** Muscimol impairs AM detection [$F_{2,6}$ = 33, P = 0.0006, n = 4; muscimol vs. baseline: t_3 = 5.6, P = 0.012; muscimol vs. saline: t_3 = 9.2, P = 0.0027]. Each point represents the average of two test days. Data from the same animal are connected by lines. Bars represent means. **(C)** Impairments were caused by reduced hit rates [$F_{2,6}$ = 69, P <0.0001; muscimol vs. baseline: t_3 = 7.7, P = 0.0045; muscimol vs. saline: t_3 = 10, P = 0.0019]. **(D)** Muscimol does not affect false alarm rates [$F_{2,6}$ = 0.50, P =0.63].

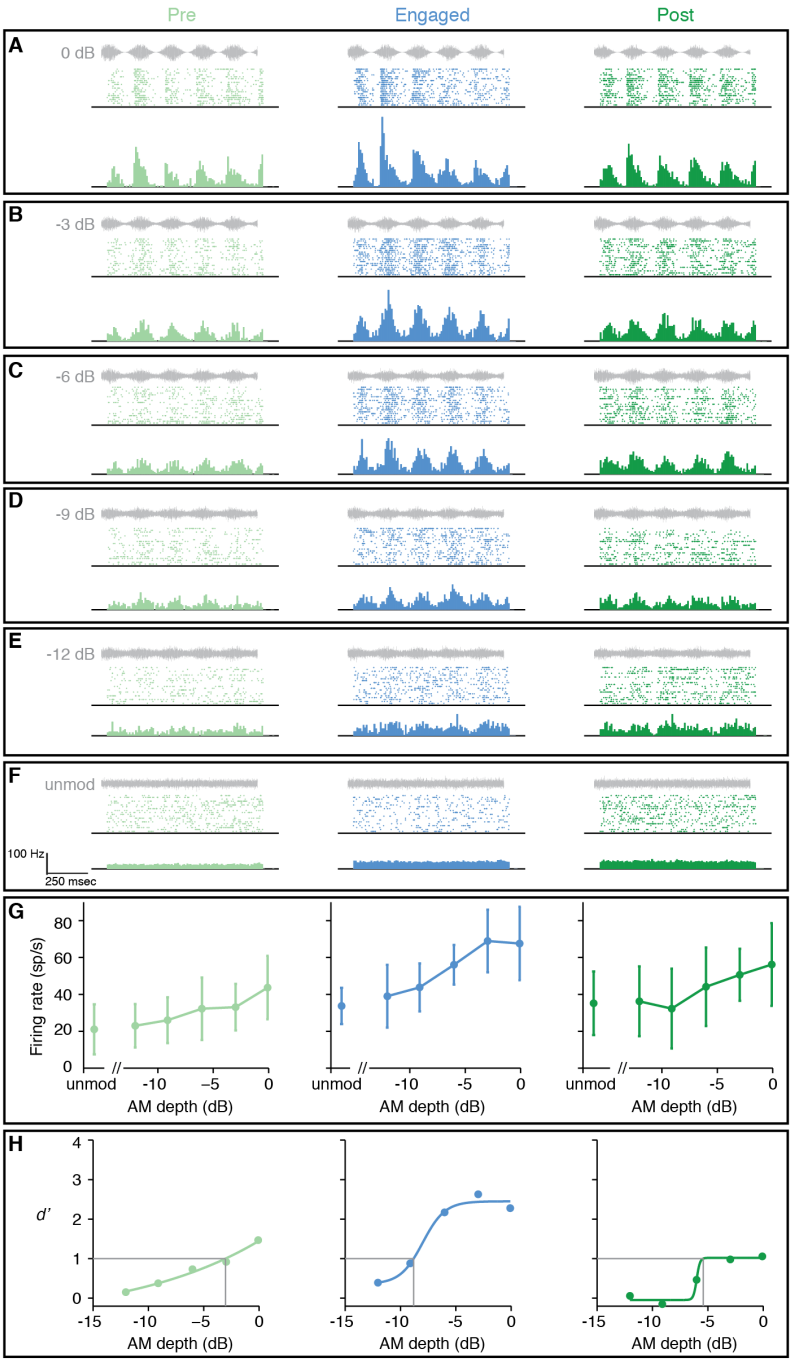

Fig S2. AM-driven activity is enhanced during task-engagement

(A-F) Rasters and post-stimulus time histograms (PSTHs) show AM-driven activity from one representative multi-unit in response to a range of AM depth stimuli. Responses were recorded on the first day of perceptual training. Grey waveforms show envelope of AM stimulus. Data are

from the same unit depicted in Fig. 3A. **(G)** The firing rate of this unit (mean ± stdev) is plotted as a function of AM depth. **(H)** The firing rate of this unit is transformed into the signal detection metric, *d'*, and plotted as a function of AM depth. Despite yielding valid thresholds during pre, engaged, and post conditions (grey lines in **H**), AM-driven activity in this unit is stronger during the engaged condition compared to the disengaged (pre and post) conditions, leading to enhanced sensitivity during task-engagement. Increased discharge rates and enhanced AM sensitivity appear to persist to some degree after task-engagement. A similar trend can be observed for the group data in Fig. 3F. This observation is consistent with previous reports of task-related ACx plasticity being maintained for hours after task completion (23-25).

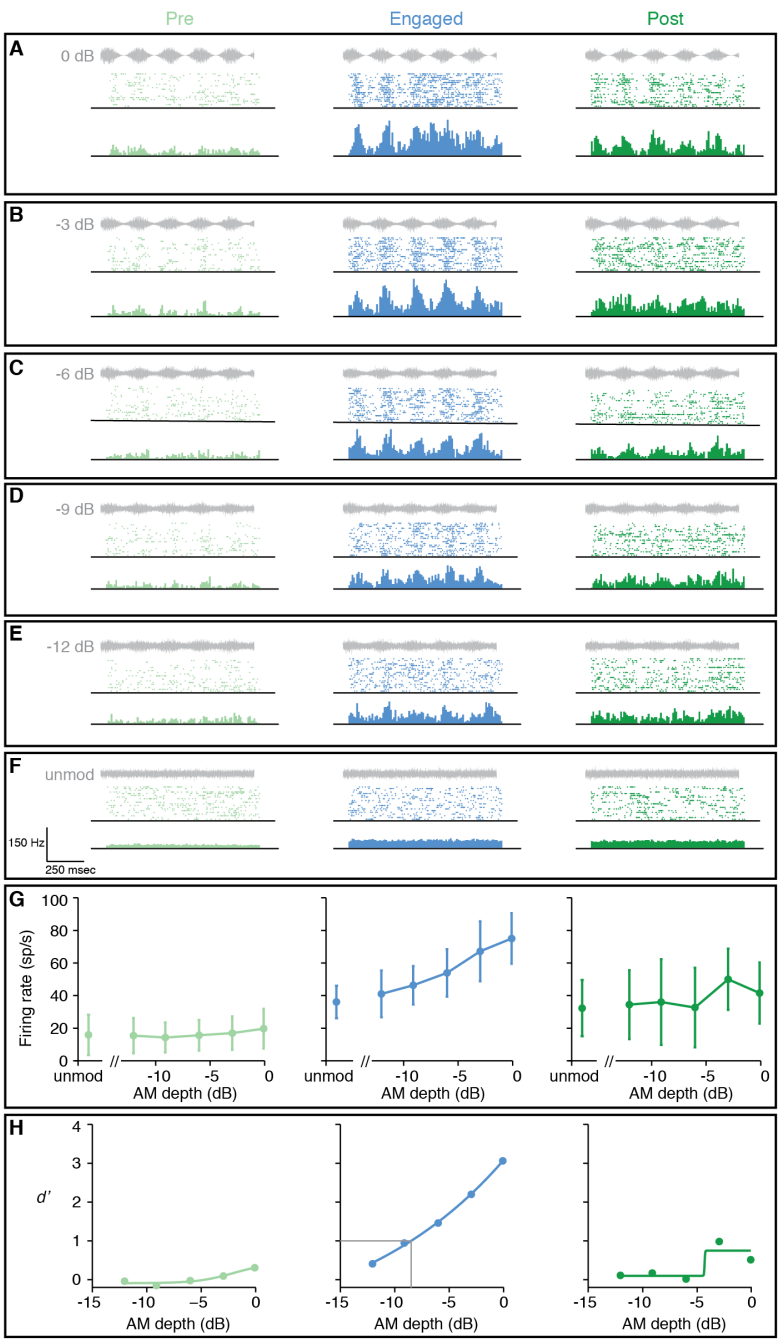

Fig S3. AM-driven activity is enhanced during task-engagement

Rasters and PSTHs (**A-F**), firing rates (**G**) and *d'* values (**H**) from another representative multi-unit from the first day of perceptual training. Plot conventions as in Fig. S2. This unit only yielded a valid threshold during task-engagement, and was therefore considered "unresponsive" to AM during pre and post conditions.

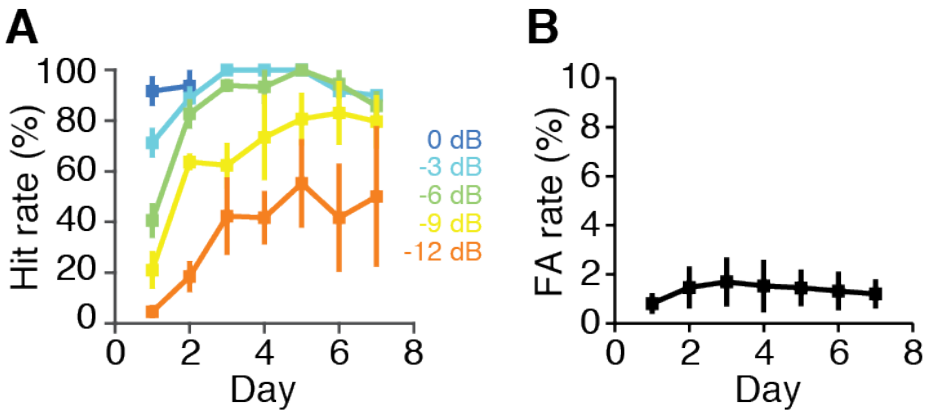

Fig. S4 Behavioral improvement is driven by increased hit rates

(A) Perceptual training increases hit rates [-3dB: $F_{6,10} = 5.3$, $P = 0.011$, $n = 4$ (days 1-3), 2 (day 4) and 1 (days 5-7); -6 dB: $F_{6,17} = 17.2$, $P < 0.0001$, $n = 4$ (days 1-3 and 5), 3 (days 4 and 6), 2 (day 7) ; -9 dB: $F_{6,19} = 4.2$, $P = 0.0075$, $n = 4$ (days 1-5), 3 (days 6-7); -12 dB: $F_{6,19} = 1.55$, $P = 0.22$; $n = 4$ (days 1-5), 3 (days 6-7)]. Note that because AM depths were systematically decreased to maintain threshold bracketing, 0 dB was only presented on the first two days. Therefore, no statistical test was performed for this stimulus value. **(B)** False alarm rates remain low throughout training [$F_{4,12} = 0.28$, $P = 0.88$; $n = 4$ animals].

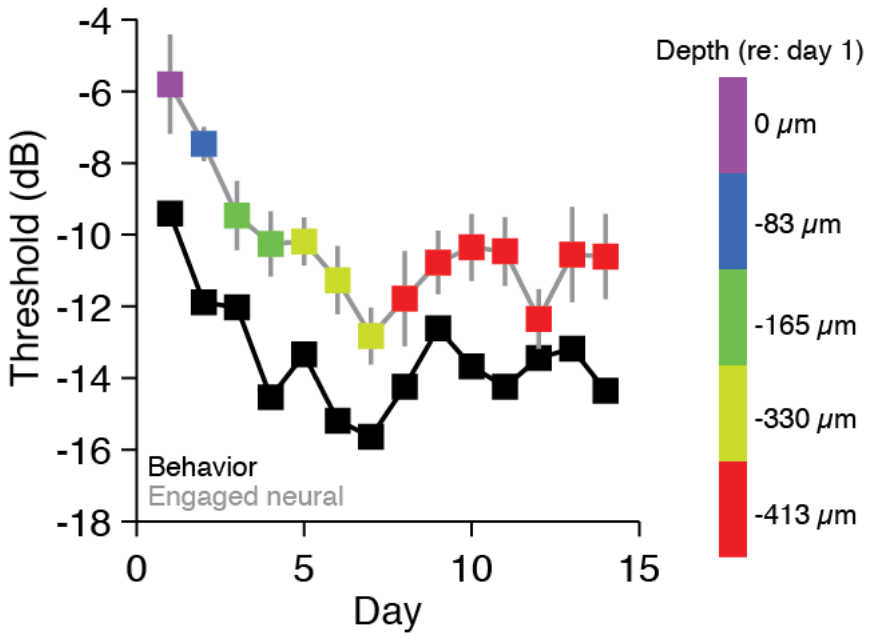

Fig. S5 Neural improvement is maintained after learning

Neural and behavioral sensitivity from one animal across 2 weeks of perceptual training. Neural thresholds improve during the first 7 days of training [Days 1-7: $F_{6,42} = 6.0$, $P = 0.0001$, $n = 49$ sites (range: 6-9/day)], and remain low during asymptotic perceptual performance [Days 7-14: $F_{7,42} = 0.81$, $P = 0.58$, $n = 50$ sites (range 4-8/day)]. Color indicates depth at which physiological data were recorded, relative to the starting depth on day 1. See Fig. S13 for histology from this same animal.

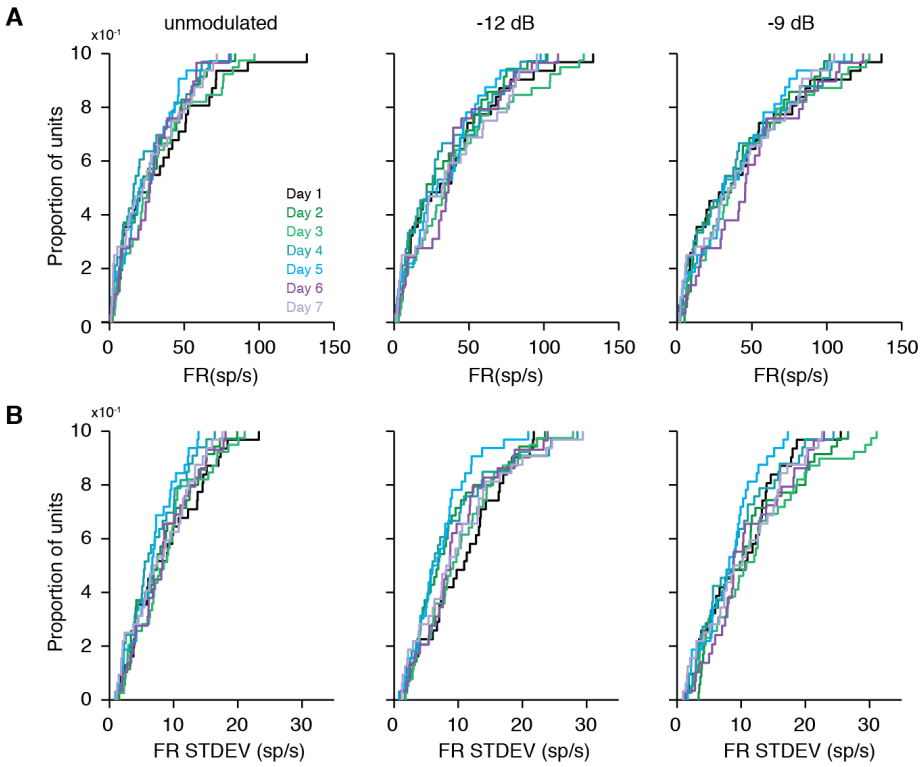

Fig. S6 Perceptual training does not affect FRs or FR STDEVs across the ACx population

(A) Population FRs do not change across training day [unmodulated: $H = 2.90$, $P = 0.821$; -12 dB: $H = 2.52$, $P = 0.866$; -9 dB: $H = 2.22$, $P = 0.899$]. **(B)** FR standard deviations also stay steady during training [unmodulated: $H = 4.58$, $P = 0.599$; -12 dB: $H = 7.82$, $P = 0.252$; -9 dB: $H = 5.52$, $P = 0.479$]. All $n = 231$ sites (range: 29-39/day; Table S1). The fact that the FR ratios of individual units increase throughout training (Fig. 2B) without a change in the global FR suggests that the day-to-day FR changes of individual units offset one another. As an example, in Fig. 2A, the FR distributions gradually separate from one another, but the day-to-day absolute FRs fluctuate in a seemingly random manner (i.e. compare where the Day 2 and Day 4 distributions fall along the *x*-axis in Fig. 2A). This finding suggests that two independent mechanisms simultaneously modulate FRs: one mechanism, induced by perceptual training,

enhances AM detection by increasing the separation of the warn and safe FR distributions. The second mechanism changes the daily FR gain on a unit-by-unit basis, in a stimulus-independent manner, possibly due to fluctuations in arousal, attention, or motivation (26, 27).

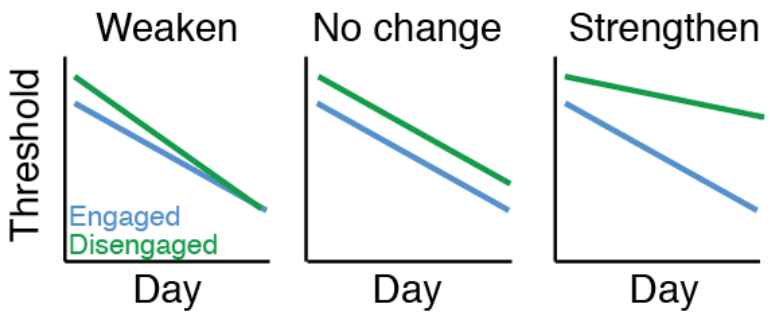

Fig. S7 Possible effects of training on a top-down process

The difference between engaged and disengaged neural thresholds reflects the strength of a top-down process. If training has no effect on this process, we would expect the magnitude of the engaged-disengaged difference to stay the same across days, despite training-based improvement (middle panel). Alternatively, if training weakens the top-down process, we would expect that the engaged-disengaged difference would gradually decrease across days (left panel). Finally, if training strengthens the top-down process, we would expect the engaged-disengaged difference to grow larger across days (right panel).

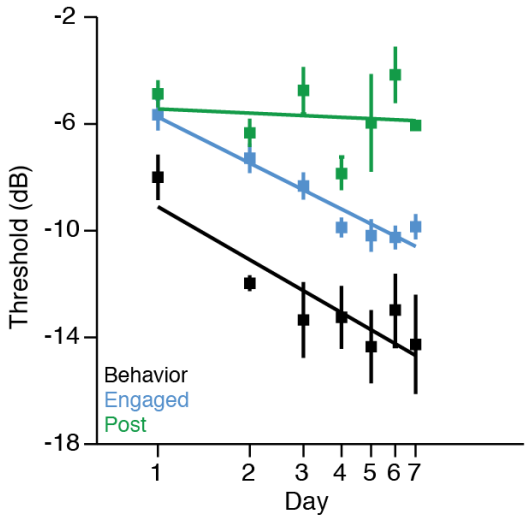

Fig S8. Behaviorally-gated neural improvement is observed using a timing-based analysis

Power was calculated from a discrete Fourier transform of spike times using a multitaper method using the Chronux toolbox for MATLAB (28, 29). This approach quantifies the magnitude of the discharge rate at the modulation rate of the AM stimulus (spikes/sec^2/Hz). As power includes both temporal and rate information in its calculation, but does not depend on stimulus phase-locking, it is a reasonable indicator of how well neural activity matches the shape of the stimulus amplitude envelope. Power values were transformed to *d'*, fit with a logistic regression, and thresholds were extracted from the fitted functions at *d'* = 1. Power-based thresholds obtained during task-engagement improved throughout perceptual training [$F_{6,171} = 10.9$, $P < 0.0001$, $n =$ 178 sites (range 22-31/day); -5.7 dB/log(day)]. Power-based thresholds obtained during disengaged listening sessions immediately following task performance ("post") did not improve [$F_{6,14} = 2.40$, $P = 0.083$, $n = 21$ sites (range 1-6/day); -0.52 dB/log(day)]. Note that the effect of training could not be assessed on thresholds from disengaged listening sessions that occurred immediately prior to task performance ("pre") because only 2 training days yielded valid power-based thresholds from more than one site.

373 **Fig. S9 Estimated spread of muscimol**

374 Representative coronal section shows spread of Fluro-Ruby (1 μL/hemisphere) 45 minutes after

375 bilateral ACx infusion.

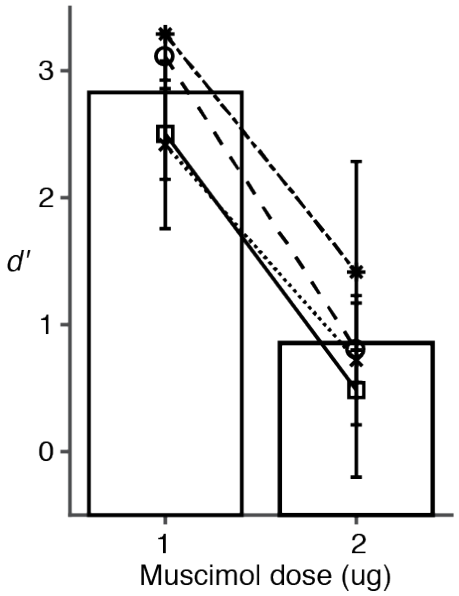

Fig S10. Dose-dependent effect of muscimol on AM detection

A high dose of muscimol (1μL/hemisphere; 1mg/mL; total dose of 2 μg) impairs detection of fully modulated (0 dB re: 100%) AM noise. A lower dose (1μL/hemisphere; 0.5 mg/mL; total dose of 1 μg) allows for excellent detection of 0 dB AM in the same animals (n = 4). Data from the same animal are connected by lines. The effect of dose was significant [t_3 = 15.29, P = 0.0006, n=4 animals]. Bars represent means. High dose (2 μg) data are replotted from Fig. S1, with each point representing the average of two muscimol sessions collected during associative testing (prior to perceptual training) on alternating days. Low dose (1 μg) data points represent the average of all *d'* values generated at 0 dB during perceptual training sessions paired with muscimol (i.e. Days 2-6 in Fig. 4A). Because AM depth values were adjusted daily to maintain threshold bracketing during perceptual training, animals were tested with 0 dB for a variable number of low-dose sessions (range: 2-4).

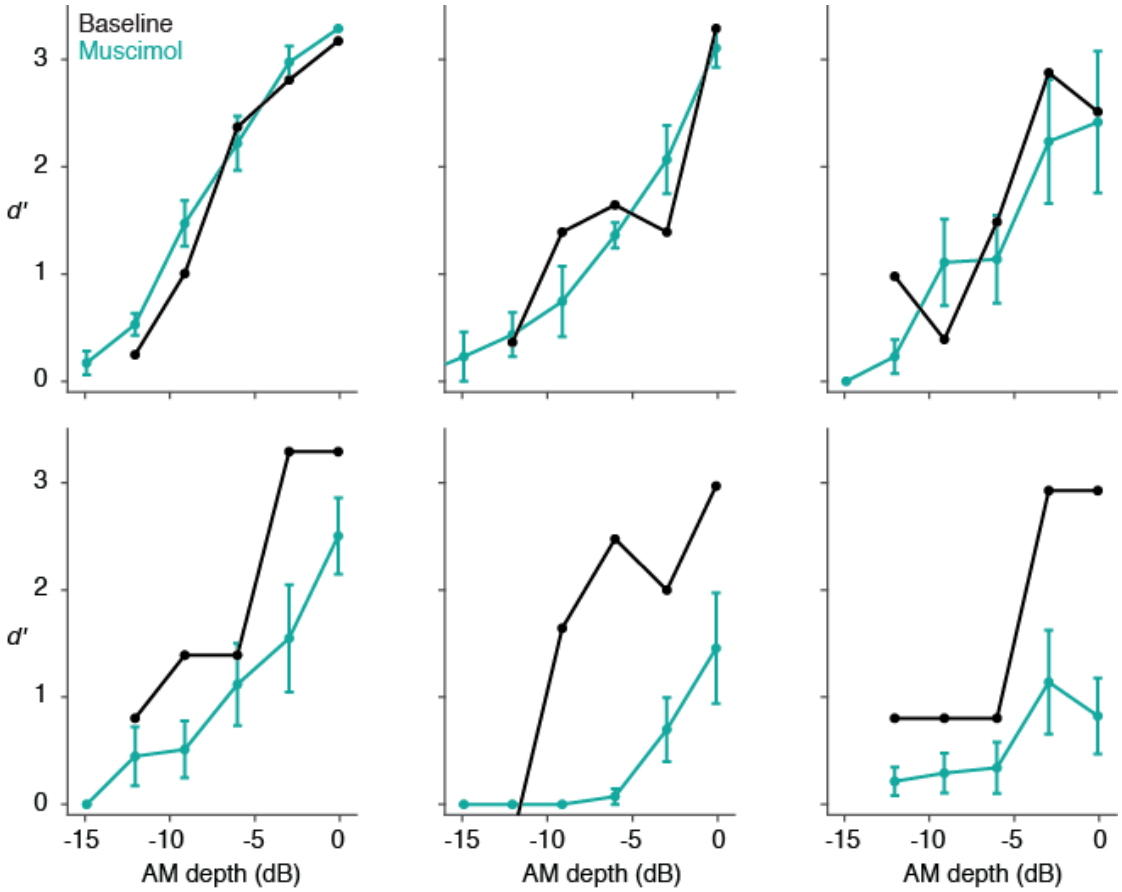

Fig S11. A low dose of muscimol does not grossly impair psychometric performance

Comparisons of psychometric performance at baseline and during muscimol training sessions. Each panel contains data from a single animal. Muscimol data are averaged across all muscimol training sessions (Days 2-6 in Fig. 4A). In general, a low dose of muscimol (0.5 mg/mL; 1μL/hemisphere; total dose of 1 μg) did not grossly perturb AM perception [$F_{1,5}$ = 5.14, P = 0.073, n = 6 animals], but did impair learning (see Fig. 4).

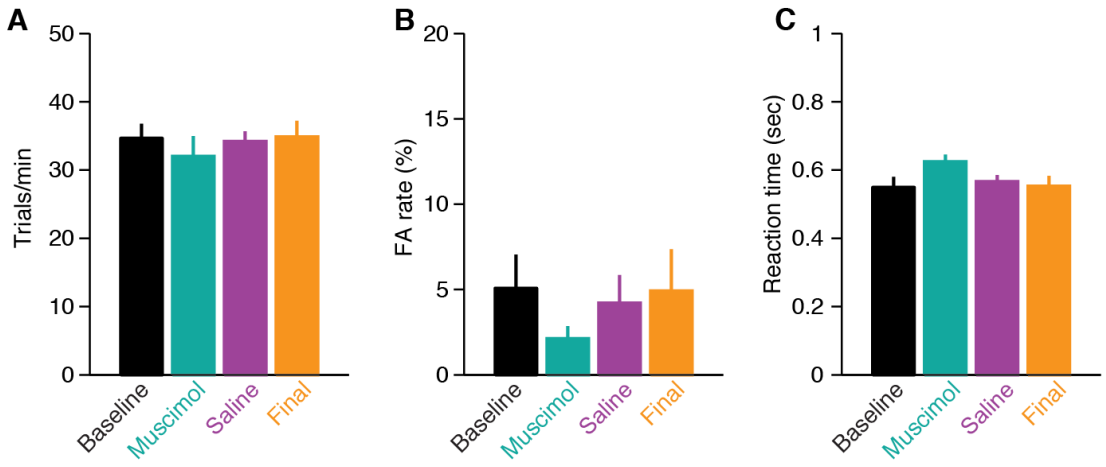

396 **Fig. S12 Muscimol-induced disruption of PL is not explained by task-specific impairments**

397 A low dose of muscimol (0.5 mg/mL, 1μL/hemisphere; total dose of 1 μg) does not affect (**A**)
398 the rate of trial completion [$F_{1.8,9.2} = 0.36$, $P = 0.69$], (**B**) false alarm rates [$F_{1.2,6.2} = 0.93$, $P =$
399 0.39], or (**C**) hit trial reaction times [$F_{3,15} = 2.2$, $P = 0.13$]. For muscimol and saline conditions,
400 across-session means were calculated for each animal. These mean values were then averaged
401 across animals to obtain the bars and sems depicted here. All $n = 6$ animals.

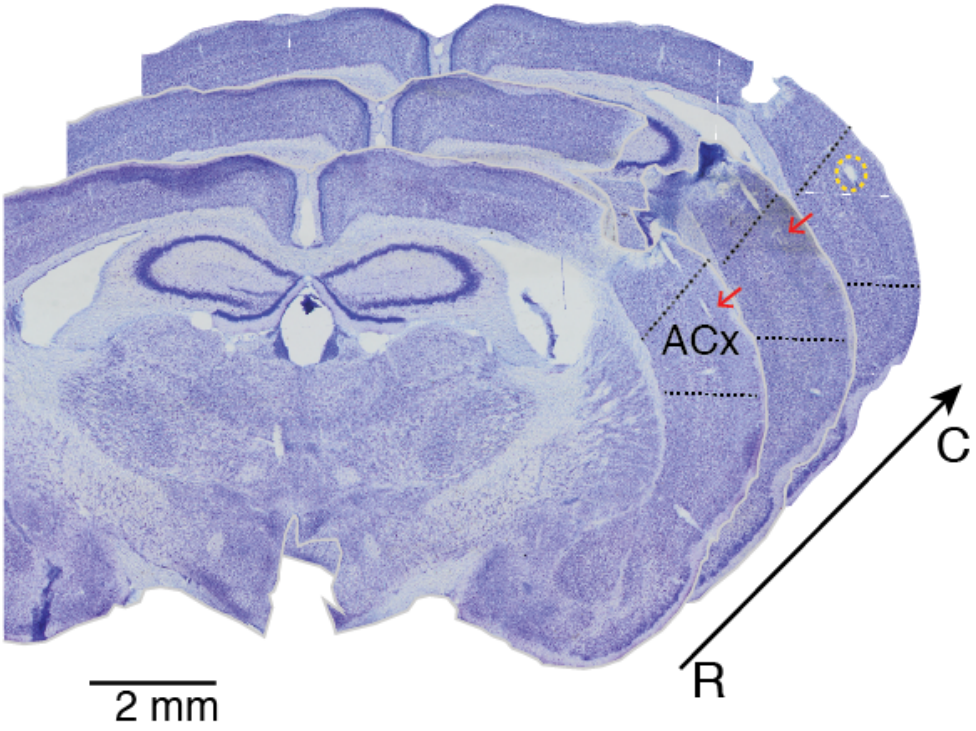

Fig. S13 Representative electrode track

Nissl-stained coronal sections from one animal arranged from rostral (R) to caudal (C) showing electrode tracks (red arrows) and electrolytic lesion (yellow circle) in ACx. Sections were separated by 180 μm.

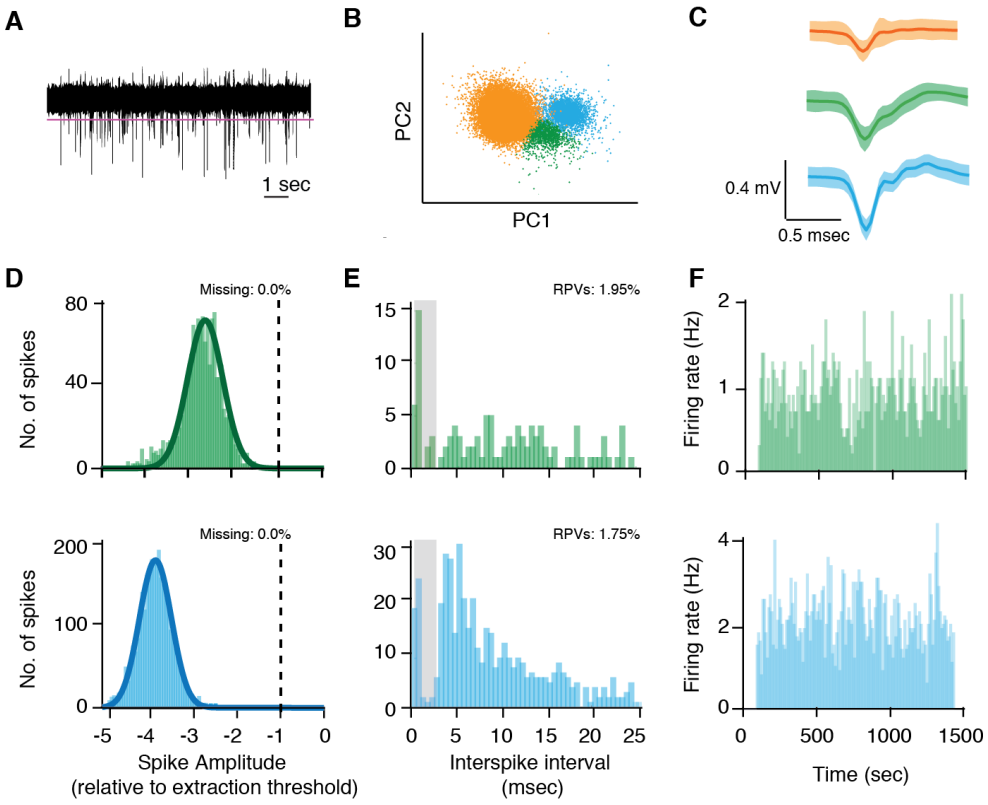

406 **Fig. S14 Spike sorting and single-unit verification**

407 **(A)** Representative voltage trace after filtering and common average referencing. Magenta line
408 indicates snippet extraction threshold. (**B**) Extracted snippets were sorted in principal component
409 (PC) space, generating **(C)** sorted waveforms (means ± 2 stdev). **(D)** Distribution of spike
410 amplitudes for the two single-units identified in **C**. Dashed vertical line represents amplitude of
411 extraction threshold. Thick line represents a Gaussian fit of the distribution, allowing for an
412 estimation of the percent of spikes missing. **(E)** Distribution of interspike-intervals for each
413 single-unit. Grey shading highlights refractory period. For both units < 2% of spikes were
414 refractory period violations (RPVs). **(F)** Firing rate histograms for each single unit over the
415 duration of the recording session. Both units show steady firing rates, demonstrating recording
416 stability.

Table S1.

Number of units responsive to AM, broken down by day and by session type.

	Pre		Engaged		Post	
Day	**Multi**	**Single**	**Multi**	**Single**	**Multi**	**Single**
1	11	0	29	2	11	1
2	6	0	32	3	5	0
3	11	0	37	2	14	0
4	4	0	33	0	7	0
5	6	0	29	3	7	0
6	2	0	28	1	4	0
7	3	1	30	2	6	0
Total	**43**	**1**	**218**	**13**	**54**	**1**

Table S2.

Within-animal correlations between behavioral and neural thresholds. AM responses during the Pre condition from subject 221955 were only observed on one day, so no correlation value could be calculated. *Significant after adjusting alpha level for multiple comparisons.

	Pre			Engaged			Post		
Subject ID	***r***	***P***	**slope**	***r***	***P***	**slope**	***r***	***P***	**slope**
217821	0.87	0.012	0.53	0.85	<0.0001*	0.74	0.39	0.23	0.32
221955	--	--	--	0.99	0.0014*	1.2	0.85	0.35	2.3
222724	0.87	0.052	1.6	0.61	0.14	0.93	0.65	0.16	1.7
222725	0.56	0.093	0.79	0.92	0.0002*	0.81	0.63	0.051	0.75

Table S3.

Within-site threshold comparisons during perceptual training (Student's paired two-tailed *t*-tests). Only units that yielded a valid threshold on both days were included in the analyses. Because some sites were lost during later sessions, the Day 1 thresholds (and the sample sizes) differ for each comparison. Data are from $n = 2$ animals. (We advanced the electrode in the remaining 2 animals throughout Days 1-5, making within-unit comparisons in those subjects impossible). *Significant after adjusting alpha level for multiple comparisons.

Comparison	Day 1 threshold (dB re: 100%) Mean ± SEM	Day N threshold (dB re: 100%) Mean ± SEM	*t*(df)	*P*	Effect size (Cohen's *d*)
Day 1 vs. Day 2	-7.0 ± 0.91	-9.9 ± 0.81	5.1(15)	0.0001*	0.65
Day 1 vs. Day 3	-6.8 ± 0.97	-9.0 ± 0.76	5.5(15)	<0.0001*	0.84
Day 1 vs. Day 4	-7.4 ± 0.99	-11 ± 0.81	8.3(13)	<0.0001*	1.2
Day 1 vs. Day 5	-7.5 ± 1.0	-13 ± 1.0	8.6(11)	<0.0001*	1.5

Table S4.

Chi-square analysis of the effect of listening condition (pre, engaged, post) on unit responsiveness to AM, broken down by day. See Table S1 for raw counts of responsive units. *Significant after adjusting alpha level for multiple comparisons.

	% Units Responsive to AM					
Day	**Pre**	**Engaged**	**Post**	**Pearson X^2**	**df**	***P***
1	23.9	67.4	26.1	23.2	2	<0.001*
2	13.0	74.5	10.6	55.6	2	<0.001*
3	20.0	69.6	25.9	34.4	2	<0.001*
4	8.50	68.8	15.2	48.3	2	<0.001*
5	12.2	65.3	14.6	41.2	2	<0.001*
6	5.00	70.7	10.0	53.0	2	<0.001*
7	9.30	71.1	14.0	48.2	2	<0.001*